(5) 475 400

63-4-4

THE JOHNS HOPKINS UNIVERSITY

DEPARTMENT OF PHYSICS

scale 1

Technical Report No. 1

CLUSTER-EXPANSION CORRECTIONS TO THE DEBYE-HŰCKEL PAIR-CORRELATION FUNCTION FOR IONIZED GASES

by Charles F. Hooper, Jr.

June, 1963

Baltimore 18, Maryland

$ 9.60

(5) 415 400

DEPARTMENT OF PHYSICS

THE JOHNS HOPKINS UNIVERSITY

BALTIMORE, MD.

Technical Report No. 1

(6) CLUSTER-EXPANSION CORRECTIONS TO THE DEBYE-HÜCKEL PAIR-CORRELATION FUNCTION FOR IONIZED GASES,

by Charles F. Hooper, Jr.

(11) June 1963, (12) 11 p.

Principal Investigator: Donald C. Kerr

NR 012-304/8-13-62

Contract Nonr 248(57)

Abstract

The Kolb-Griem theory of spectral line broadening occurring in plasmas is discussed; emphasis is placed on the importance of the electric microfield distribution. The Mozer-Baranger calculation of the electric microfield distribution in a plasma is outlined; its dependence upon the nature of the component particle correlations is shown. The electrons and ions must be treated separately because of their inherent differences; the electrons interact through a Coulomb field, whereas the ions interact with shielded fields. The Salpeter cluster-expansion technique is considered in detail. It is applied to the determination of pair correlation functions and the corresponding potentials of mean force for both Coulomb and shielded fields. The calculations are made up to second order in complexity. Corrected expressions for the potentials of mean force are compared with the corresponding Debye-Hückel results. Significant differences are found; this is particularly true for the shielded-field cases. It is demonstrated that use of the corrected pair-correlation functions in the Mozer-Baranger microfield calculation could significantly alter the results. The possibility of including such corrected results in the line-broadening theory is considered; it is indicated that the influence of these corrections on the profile of the Lyman-β line should be experimentally observable.

Acknowledgments

It is a pleasure to acknowledge the support of Professor Donald E. Kerr. His encouragement throughout the duration of this work has served to make this research both profitable and enjoyable. I am no less indebted to Professor Hans R. Griem of the University of Maryland for many helpful discussions; his insight into the problems involved in this work has proved invaluable.

I would like to thank Aircraft Armaments, Inc., of Cockeysville, Maryland, for making available their LGP-30 computer. Particularly deserving of thanks are Mr. A. G. Patterson and Mr. M. F. Wilt, who have provided valuable assistance with the computer calculations. I wish also to thank Mrs. T. Netro for her cheerful help with the preparation of this manuscript.

Financial support from the Office of Naval Research is gratefully acknowledged.

TABLE OF CONTENTS

TABLE OF CONTENTS (Cont'd)

I. INTRODUCTION

The theory of spectral line broadening has recently[5][6] been improved to the point where the profiles of both overlapping and isolated spectral lines, arising from hydrogen and helium plasmas, are well understood. Two features of these spectral lines are frequently of special interest: the line half width and the line shift. The first of these quantities, together with the entire line profile is theoretically predicted to within 10% of the experimentally determined values. However, the spectral line shift is generally not in agreement with experiment; deviations of better than 30% are frequently found.[46] Furthermore, these variations are not always in the same direction. It therefore remains to explain these shifts satisfactorily.

In the construction of the general line-broadening theory, numerous approximations have been made. A review of the underlying assumptions leads to the conclusion that the most probable causes of the shift discrepancy are: (1) the crude treatment of strong electron collisions, (2) the use of the Debye-Hückel pair-correlation function in the calculation of the electric microfield distribution, (3) the approximate treatment of ion perturbations in the cases where the present theory is not adequate.[51] Although these quantities will be discussed in detail in succeeding chapters, it may be mentioned here that the pair distribution function specifies the spatial distribution of two interacting particles, while the electric microfield distribution function determines the spatial characteristics of the electric field in a plasma. Thus, the electric field perturbs the radiating atom and therefore influences the nature of the radiation itself. It is known that in some instances the line shift

is particularly sensitive to the electric field distribution; thus, a method of checking these distributions is available.

Current theories of line broadening rely on the Debye-Hückel distribution function[1] for both the Coulomb and shielded fields. However, as will be indicated later, the assumptions necessary in the derivation of this function are not applicable to many plasmas of interest. It is the purpose of this thesis to calculate the pair distribution function for the Coulomb and shielded electric fields, to consider in detail the various orders of correction, and finally to indicate what significance, if any, the deviations from the Debye-Hückel results have as related to the shift of spectral lines.

For the purpose of this investigation, it is necessary to specify a particular plasma model. The one chosen eliminates infinitely attractive potentials from consideration. The electrons are treated as negatively charged particles in a uniformly neutralizing background, and the ions are assumed to be shielded by electron clouds which travel permanently with them. That such a model is applicable to practical plasma problems may not be immediately apparent; further discussion and justification will be presented in Chapter III.

The motivation for choosing this particular model stems from the work of Mozer and Baranger[1], which describes a clever method for calculating the electric microfield. The Baranger approach utilizes a cluster-expansion program which is reminiscent of the well known Mayer cluster development. Particle correlations are included in this theory as a perturbation expansion: the first group of terms contain the 1-body or independent correlation functions, the second group the 2-body or pair-correlation

functions, etc. For such a process to be valid, increasing orders of correlation must become very small, in a perturbation sense. Although both the electrons and ions contribute to the electric microfield, they do so in a very different manner; in view of this difference, discussed in Chapter III, the two contributions are handled separately. The relation of the corrected correlation functions to the Mozer-Baranger theory will be considered later.

In order to effect the desired correction to the pair distribution function, the method proposed by Salpeter[2] is used. This procedure has previously been applied by Bowers[52] to calculate the Coulomb potential of the mean force; however, since we consider several aspects of this work to be incorrect, the present work reverts to (2) as primary reference. The Salpeter technique embodies one of the cluster-expansion methods frequently used in statistical mechanics. It differs from most other approaches in that it is designed for use with systems of particles having long-range interaction potentials. Although the most notable of these is the Coulomb potential, the method should also be useful when dealing with potentials which are long-range, but finite. The applicability criterion is that the potentials involved should have ranges equal to or greater in magnitude than the average particle separation, given by $r_o \cong \rho^{-1/3}$ (ρ = particle density). In the cases to be considered here, this requirement is satisfied; it is automatically satisfied for the Coulomb case, and for the shielded potential it is also valid in the range of densities and temperatures of interest to most plasma line broadening applications. Another aspect of this proposed correction

procedure is that it involves corrections which refer to particle configurations: The first term of the pair-correlation function considers the most simple clusters of interacting particles; the second correction takes the next most simple configurations and so on. The details of this expansion technique are dealt with in Chapter IV.

The corrected distribution function is studied as a function of particle density and temperature. It is shown that in the given range of parameters, the second order (complexity) contribution is much less than the first order term. However, the deviation of the new functions from those predicted by Debye-Hückel theory will be shown to be quite large in some cases. In light of this last disclosure, the expected influence of the corrected pair-correlations functions on the microfield distribution is considered and the need for a revised calculation is indicated.

To summarize: In Chapter II some aspects of line-broadening theory will be discussed in an attempt to point out further the motivation for the problem. Chapter III deals with the electric microfield calculations of Baranger and Mozer and indicates the importance of the pair-distribution function in this respect. Salpeter's technique of calculating the pair-distribution function will be the subject of Chapter IV, and its application to both the shielded and Coulomb cases is covered in Chapter V. Chapter VI will present the conclusions of this study, together with recommendations for future work.

II. SOME ASPECTS OF LINE-BROADENING THEORY

From 1958 to 1962, H. R. Griem, A. C. Kolb, and M. Baranger developed a theory of spectral line broadening in hydrogen and helium plasmas. This theory pointed out the importance of electron broadening and provided a coherent treatment of the joint electron-ion contribution to the resultant spectral line profile.

The approach is simply this: electrons and ions, treated as classical particles, perturb a radiating atom, thereby influencing the intensity distribution of the resulting radiation. Looking more closely at the procedure one sees that in general, three steps are followed:

(1) The radiating atom is assumed to lie in a static electric field, E, created by the ions, and hence is subject to Stark splitting.

(2) Electron broadening of the resultant sharp lines is treated by the impact approximation.

(3) The electron-broadened spectrum is averaged over the probability distribution of the electric field.

Step (1) amounts to the usual Stark effect, where the electric field E is calculated for a particular ion configuration.

In carrying out step (2), the electrons are treated in the classical-path approximation. In order to justify this assumption that the electrons may be treated as classical particles with straight-line trajectories, one must state that the momentum transfer in such an impact perturbation is small, i.e., $\frac{\Delta P}{P} \ll 1$ where ΔP momentum transfer and P = initial momentum. Another necessary restriction is that the perturber wave-packet dimension, ΔX, be small compared with the impact parameter, ρ. Thus, it is seen that we are dealing with interactions which

on the average are weak and long range.

The third step requires that an electric microfield distribution be calculated for the plasma model previously introduced.

Fig. 1 illustrates: (a) the nature of the classical-path approximation, and (b) the type of overlapping spectral line handled by this theory

(a)

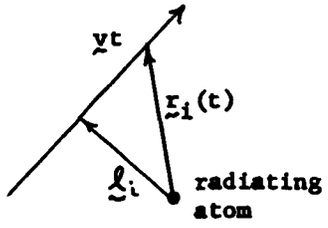

$\tau \sim \frac{\ell}{v}$ is referred to as the collision time.

$\underset{\sim}{r}_i(t) = \underset{\sim}{\ell}_i + \underset{\sim}{v}_i t$

where $\underset{\sim}{r}_i(t)$ is the position vector of the i th electron relative to the radiating system.

(b)

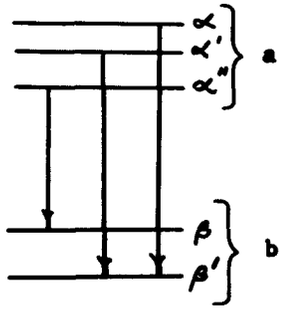

where a (α, α', α'') represents an initial level with principal quantum no. "a" and substates α, α', α'' and b (β, β') represents the corresponding final states.

Figure 1.

The transition between level a(α , α', α'') $\longrightarrow$ b(β , β') may give rise to a complicated intensity distribution such as that shown in Fig. 2.

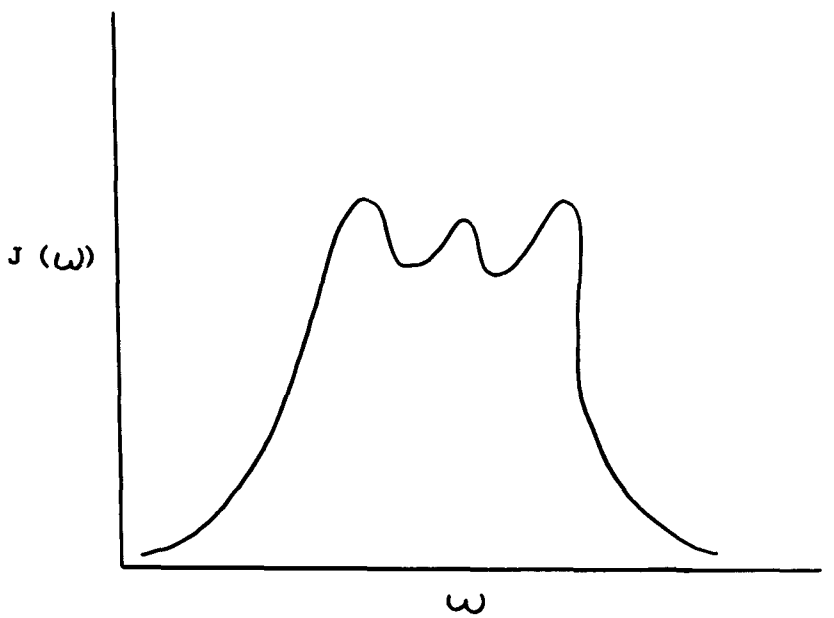

Figure 2. Spectral Line Intensity Distribution

It is possible to derive an expression for the spectral intensity distribution function for a quantum-mechanical radiating system with time-dependent dipole moment, $\mu(t)$ assuming an equilibrium situation.[14] The final expression for this quantity is

$$J(\omega) = \frac{2\omega^4}{3\pi c^2} \quad \text{Tr} \quad \text{Re} \int_0^\infty dt \; e^{i\omega t} \rho_e \left\{ \mu(t)\mu(0) \right\}_{\text{average}} \qquad (2.1)$$

where

$J(\omega)$ = Spectral Intensity

ω = Angular Frequency

c = Speed of Light

t = Time

ρ_o = Boltzman Factor = $Z^{-1} e^{-\beta (H_o + V(t))}$

Z = Partition Function

$\beta = k T$

k = Boltzman Constant

T = Temperature in degrees Kelvin

H_o = Unperturbed Hamiltonian

$V(t)$ = Time-Dependent Perturbation

$\mu(t)$ = Dipole moment of the radiating atom at time (t)

$\{\ \}_{AVG.}$ = Average over all perturber configurations.

The average specified in Eq. (2.1) refers to the average over all possible perturber collisions, e.g., over all values of: (1) impact parameter; (2) perturber velocity; (3) collision angles; and (4) collision time. This averaging process is necessary because $\{\mu(t)\,\mu(0)\}$ is always calculated for a particular instantaneous perturber configuration.[14] Since the interaction is considered weak, it is assumed in the following that $V(t) << H_o$ or that

$$\rho_o \cong Z^{-1} e^{-\beta H_o} \qquad (2.2)$$

Thus ρ_o is independent of time and may be taken outside the integral giving (aside from a constant factor)

$$J(\omega) = \rho_o \ \mathrm{Tr}\ \mathrm{Re} \int_0^\infty dt\ e^{i\omega t} \left\{ \mu(t)\, \mu(0) \right\}_{\text{average}} \qquad (2.3)$$

The problem now is the calculation of $\left\{ \mu(t)\mu(0) \right\}$. This function is frequently referred to as the auto-correlation function; if the dipole moment of the radiating atom is $\mu(t)$, and further, if the perturbing interactions serve to damp the dipole moment, there exists a correlation time, T_c, past which the time integral over the correlation function fast approaches zero. The correlation time then sets practical limits on the time integration performed in the evaluation of $J(\omega)$ and thus represents a measure of the radiating system "memory". In general, it is not possible to determine this function; fortunately, there are two special cases when a solution, using established techniques, can be obtained. These are:

(1) The collision time $\tau \gg T_c$, the correlation time;

(2) The collision time $\tau \ll T_c$, the correlation time.

The first case, (1), is referred to as the quasi-static approximation. Here the collision is so strong that it completely disrupts the phase of the radiating system in a time short compared to the collision time, τ; the disruption takes place so rapidly that it may be assumed that the perturbing particles (ions) remain fixed during τ. This first approximation is useful for dealing with ion perturbations over major portions

of most spectral line profiles. It is particularly good in regions well removed from the center of the line; this of course is true because of its strong-collision nature.

In the second case, the impact approximation is applicable; here many collisions are necessary before the phase of the radiating system is completely disrupted. This implies that interactions treated in this approximation are on the average weak. Electrons are very successfully handled with this technique everywhere but on the far wings of the profiles; it may also be used in some instances to determine ion contributions at the center of the line.

The quasi-static approach is used to accomplish step (1) and the impact approximation is used in step (2). Hence, at the end of these first two steps, we have an expression for the spectral intensity which is a function of both the frequency ω and a fixed value of the electric microfield, E:

$$J(\omega, E) = \frac{w}{\pi} \left[w^2 + (\omega - d - C(E))^2 \right]^{-1} \qquad (2.4)$$

where: w = line half-width as determined from step (2).

d = line shift as determined from step (2).

C(E) = a function of the field strength E; it is proportional to E for the linear Stark effect and to E^2 for the quadratic Stark effect.

In order to find the intensity distribution $J(\omega)$, it is necessary to average $J(\omega, E)$ over a suitable electric microfield distribution, W (E).

Therefore,

$$J(\omega) = \int_0^\infty W(E)\, J(\omega, E)\, dE \qquad (2.5)$$

or,

$$J(\omega) = \frac{w}{\pi} \int_0^\infty \frac{W(E)\, dE}{w^2 + (\omega - d - C(E))^2} \qquad (2.6)$$

Recall that the function W (E) gives the probability of finding an electric field of magnitude E, at a particular spatial point which we choose to be the radiating system. This function is strongly dependent upon the specific characteristics of the particle correlations. The exact nature of the dependence is shown in the next chapter.

III. THE ELECTRIC MICROFIELD DISTRIBUTION FUNCTION

A. Introduction

The last chapter indicated that when the quasi-static approximation was applicable the perturbers involved may be considered to produce a time-independent electric field. To arrive at an electric microfield distribution function, one must average over all possible perturber configurations or, what amounts to the same thing, over the possible electric fields.

Holtsmark[4] first calculated this distribution function for a gas of charged particles; however, in doing so he neglected to account for the fact that charged particles interact with one another and hence are strongly correlated. He determined the probability of finding a particular electric field E, due to a static random distribution of singly charged ions, in a specific range, $E_o < E < E_o + d E$. Such a development represents a strong-collision theory, since it neglects the weaker but highly probable perturbative interactions where correlations are important. Therefore, it is not surprising that the Holtsmark theory incorrectly describes the center of spectral lines, but gives much better results when applied to line wings. This theory will also be briefly mentioned in Chapter IV.

Since this initial work, others have attempted to improve on the theory of electric microfield distributions; the primary effort has been to correctly include particle correlation. Ecker[17], and Hoffman and Theimer[18], followed the Holtsmark procedure of assuming statistical independence, but replaced the Coulomb field with a shielded field. Broyles[20] uses the Bohm-Pines collective-coordinate technique by considering short and long range interactions separately in his evaluation of the microfield distribution at a radiating ion. Margenau and Lewis[21] also consider the

electric field at an ion due to perturbing ions, but neglect the inter-ion interaction. This last method also has the disadvantage of not being applicable to neutral atoms. Although this criticism is not true of the Broyles' approach, it should be pointed out that his expression for the microfield distribution, in the limit T approaches infinity, does not reduce to the expected Holtsmark result.

In two papers,[1] Mozer and Baranger put forward a new method of including correlations in the calculation of the electric microfield distribution functions. The construction of this theory involves a perturbation expansion and has the desirable feature of reducing to the Holtsmark result in the limit where T approaches infinity. To be practical, we must restrict its use to plasmas where the interaction energies are considerably less than the thermal energies, i.e., less than kT. It is possible to calculate all orders of correlation, but only the two-body example is developed in detail.

The actual calculation of the microfield distribution function will involve the Fourier transform of the distribution function rather than the function itself; here, as in many instances, the transform is easier to handle. In the following work, E, refers to an arbitrary electric field; it will later be used to refer to both the Coulomb and shielded fields. Following the notation of Mozer and Baranger, we refer to the collective electron field as the high-frequency field, and the resultant ion field is termed the low-frequency field.

B. The Mozer-Baranger Theory[1]

Consider a volume V with a given number of particles N, the coordinates of which are $\underset{\sim}{r}_1$, $\underset{\sim}{r}_2$, ... $\underset{\sim}{r}_n$; the particle density is given

by $\rho = \frac{N}{V}$. Furthermore, it is assumed that thermal equilibrium conditions prevail. The quantity to be calculated, $W(\underset{\sim}{E})$, gives the probability of finding a total electric field E in a range $\underset{\sim}{E}$ to $\underset{\sim}{E} + d\underset{\sim}{E}$ at a given point in space. It is usually convenient to take this point as the origin of the coordinate system. The Fourier transform of the field distribution function is

$$F(\underset{\sim}{k}) = \int e^{i\underset{\sim}{k}\cdot\underset{\sim}{E}} W(\underset{\sim}{E})\, d^3 E \qquad (3.1)$$

where the field E at the origin is equal to

$$\underset{\sim}{E} = \sum_{i=1}^{N} \underset{\sim}{E}_i$$

$\underset{\sim}{E}_i$ = field produced by one of the particles located at point $\underset{\sim}{r}_i$. Now it is well known that Eq. (3.1) may also be expressed in terms of the particle distribution function $P(\underset{\sim}{r}_1, \cdots \underset{\sim}{r}_N)$. Thus, we replace $W(\underset{\sim}{E})\, d^3 E$ in the Fourier transform by $P(\underset{\sim}{r}_1 \cdots \underset{\sim}{r}_N)\, d^3 r_N$ where $P(\underset{\sim}{r}_1 \cdots \underset{\sim}{r}_N)$ gives the probability of finding the N particles in a particular configuration. For a classical gas in thermal equilibrium, $P(\underset{\sim}{r}_1 \cdots \underset{\sim}{r}_N)$ is the Boltzmann distribution,

$$P(\underset{\sim}{r}_1 \cdots \underset{\sim}{r}_N) = \frac{e^{-\beta U(\underset{\sim}{r}_1 \cdots \underset{\sim}{r}_N)}}{\int\cdots\int_{\text{volume}} e^{-\beta U(\underset{\sim}{r}_1 \cdots \underset{\sim}{r}_N)} \prod_{i=1}^{N} d^3 r_i} \qquad (3.2)$$

Here, we have defined

$$d^3r_1 \cdots dr_N^3 = \prod_{i=1}^{N} d^3 r_i$$

With the above substitution, Eq. (3.1) becomes

$$F(\underset{\sim}{k}) = \int \cdots \int e^{i\underset{\sim}{k} \cdot (\underset{\sim}{r}_1 + \cdots + \underset{\sim}{r}_N)} P(\underset{\sim}{r}_1 \cdots \underset{\sim}{r}_N) \prod_{i=1}^{N} d^3 r_i \qquad (3.3)$$

Using a trick similar to that employed in the usual cluster-expansion procedure, we may write:

$$e^{i\underset{\sim}{k} \cdot \underset{\sim}{r}_i} = e^{i\underset{\sim}{k} \cdot \underset{\sim}{r}_i} - 1 + 1 \qquad (3.4)$$

$$= \varphi_i + 1$$

Substitution of this expression into equation (3.3) gives:

$$F(k) = \int \cdots \int \left[1 + \sum_i \varphi_i + \sum_{i<j} \varphi_i \varphi_j + \cdots\right] P(\underset{\sim}{r}_1 \cdots \underset{\sim}{r}_N) \prod_{i=1}^{N} d^3 r_i \qquad (3.5)$$

$$= F_o(\underset{\sim}{k}) + F_1(\underset{\sim}{k}) + \cdots + F_M(\underset{\sim}{k}) + \cdots \qquad (3.5a)$$

where

$$F_M(k) = \int \cdots \int \sum_{i<j<\cdots<M} \varphi_i \varphi_j \cdots \varphi_M P(\underset{\sim}{r}_1 \cdots \underset{\sim}{r}_M) \prod_{i}^{M} d^3 r_i \qquad (3.5b)$$

Since $P\ (\underset{\sim}{r}_1 \cdots \underset{\sim}{r}_N)$ is symmetric with respect to an interchange of particle coordinates, it is permissible to write $F_m\ (\underset{\sim}{k})$ as

$$F_M\ (\underset{\sim}{k}) = \frac{N!}{M!\,(N - M)!} \int \cdots \int \varphi_1 \cdots \varphi_M\, P_N\ (\underset{\sim}{r}_1 \cdots \underset{\sim}{r}_N) \prod_{i=1}^{N} d^3 r_i \qquad (3.6)$$

Note that in this expression it is possible to integrate over all but the specified M particle coordinates thus obtaining a new probability function P_M which depends only on the M coordinates $(\underset{\sim}{r}_1 \cdots \underset{\sim}{r}_M)$, and is equal to V^{-M} times the M-body correlation function. Hence, we write:

$$F_M\ (\underset{\sim}{k}) = \frac{N\ !}{M!\,(N - M)!} \int \cdots \int \varphi_1 \cdots \varphi_M\, P_M\ (\underset{\sim}{r}_1 \cdots \underset{\sim}{r}_M) \prod_{i=1}^{M} d^3 r_i \qquad (3.7)$$

P_M can now be expanded in a perturbation series involving increasing orders of correlation.[50] Thus, the first term contains only theproduct of one-body or independent probability functions; the second term involves the two-body interaction corrections, while each successive term includes corrections involving one more particle added to the particle cluster. To illustrate:

$$V^3 P_3 = s_1\ (\underset{\sim}{r}_1) s_1 (\underset{\sim}{r}_2) s_1 (\underset{\sim}{r}_3) + s_1 (\underset{\sim}{r}_1) s_2 (\underset{\sim}{r}_2, \underset{\sim}{r}_3) + s_1 (\underset{\sim}{r}_2) s_2 (\underset{\sim}{r}_1, \underset{\sim}{r}_3) \qquad (3.8)$$

$$+ s_1 (\underset{\sim}{r}_3) s_2 (\underset{\sim}{r}_1, \underset{\sim}{r}_2) + s_3 (\underset{\sim}{r}_1, \underset{\sim}{r}_2, \underset{\sim}{r}_3)$$

where $s_1(\underset{\sim}{r}_i)$ represents the one-body or independent probability function, s_2 is the two-body correlation function, and so on. Since the s functions are also symmetric with respect to an interchange of particle coordinates, $F_M(k)$ becomes

$$F_M(k) = \frac{N!}{M!\,(N-M)!} \int \cdots \int \varphi_1 \cdots \varphi_M \, P_M(\underset{\sim}{r}_1 \cdots \underset{\sim}{r}_M) \prod_{i=1}^{M} d^3 r_i$$

$$= \frac{N!}{M!} \frac{V^M}{(N-M)!} \left\{ C(M)_{1 \cdots 1} \int \cdots \int \prod_{i=1}^{M} \varphi_i \, s_1(\underset{\sim}{r}_i) \, d^3 r_i \right.$$

$$+ C(M)_{1 \cdots 1,2} \int \cdots \int \prod_{j=3}^{M} s_1(\underset{\sim}{r}_j) \, s_2(\underset{\sim}{r}_1, \underset{\sim}{r}_2) \prod_{i=1}^{M} \varphi_i \, d^3 r_i$$

$$+ C(M)_{1 \cdots 1,\,2,\,2} \int \cdots \int \prod_{j=5}^{M} s_1(\underset{\sim}{r}_j) s_2(\underset{\sim}{r}_1, \underset{\sim}{r}_j) s_2(\underset{\sim}{r}_3, \underset{\sim}{r}_4) \prod_{i=1}^{M} \varphi_i \, d^3 r_i \quad (3.9)$$

$$+ \cdots$$

$$+ C(M)_{1 \cdots 1,\,3} \int \cdots \int \prod_{j=4}^{M} s_1(\underset{\sim}{r}_j) \, s_3(\underset{\sim}{r}_1, \underset{\sim}{r}_2, \underset{\sim}{r}_3) \prod_{i=1}^{M} \varphi_i \, d^3 r_i$$

$$+ C(M)_{1 \cdots 1,2,3} \int \cdots \int \prod_{j=6}^{M} s_1(\underset{\sim}{r}_j) s_2(\underset{\sim}{r}_1, \underset{\sim}{r}_2) s_3(\underset{\sim}{r}_1, \underset{\sim}{r}_2, \underset{\sim}{r}_3) \prod_{i=1}^{M} \varphi_i \, d^3 r_i$$

$$\left. + \cdots + \cdots \right\}$$

The coefficients $C(M)_{\mu_i \cdots \mu_i, \cdots, \mu_r \cdots \mu_r}$ are numbers equaling the number of ways to choose distinct groups of $\mu_i, \mu_j, \cdots, \mu_l$ particles out of a total of M identical particles, with $\mu_i < \mu_j < \cdots < \mu_l$. Distinct groups implies that all the particles of a specific group are different from all particles of any other group. In general, if there are $\lambda_i \mu_i$, $\lambda_j \mu_j$ etc., with the condition that $\lambda_i \mu_i + \lambda_j \mu_j + \cdots + \lambda_r \mu_r = M$, the coefficient is

$$C(M)_{\mu_i \cdots \mu_i, \cdots, \mu_r \cdots \mu_r, \cdots} = \frac{M!}{\lambda_i! \, (\mu_i!)^{\lambda_i} \cdots \lambda_r! \, (\mu_r!)^{\lambda_r} \cdots} \quad (3.10)$$

One can define a quantity $h_{\mu_i}(k)$ as

$$h_{\mu_i}(\underset{\sim}{k}) = \int \cdots \int \varphi_1 \varphi_2 \cdots \varphi_{\mu_i} \, s_{\mu_i} \, (\underset{\sim}{r}_1 \cdots \underset{\sim}{r}_{\mu_i}) \prod_{j=1}^{\mu_i} d^3 r_j \quad (3.11)$$

With this definition, the Fourier transform of the field distribution, in the limit as N and V approach infinity, while the density $\rho = \frac{N}{V}$ remains constant, is

$$F(\underset{\sim}{k}) = \sum_{M=o}^{\infty} \frac{\rho^M}{M!} \left[\sum_{\substack{\text{all partitions} \\ \text{of M}}} C(M)_{\mu_i \cdots \mu_i, \cdots, \mu_r \cdots \mu_r} \, h_{\mu_i}^{\lambda_i}(\underset{\sim}{k}) \cdots h_{\mu_r}^{\lambda_r}(\underset{\sim}{k}) \right] \quad (3.12)$$

$$= \prod_{\mu_i = 1}^{\infty} \sum_{\lambda_i = 0} \left[\frac{\rho^{\mu_i}}{\mu_i!} \, h_{\mu_i}(\underset{\sim}{k}) \right]^{\lambda_i} \frac{1}{\lambda_i!}$$

$$= \prod_{\mu_i = 1}^{\infty} \exp \left[\frac{\rho^{\mu_i}}{\mu_i!} \, h_{\mu_i}(\underset{\sim}{k}) \right]$$

$$= \exp\left[\sum_{\mu_i=1}^{\infty} \frac{\rho^{\mu_i} h_{\mu_i}(\underset{\sim}{k})}{\mu_i !}\right]$$

This expression for F (k) is one frequently found in the conventional cluster expansions[50], an exponential of a power series where successive terms contain higher-order clusters. It can be shown that in the high-temperature limit only h_1 (k) remains and that

$$F(\underset{\sim}{k}) = e^{\rho h_1(\underset{\sim}{k})}$$

$$\xrightarrow{T \to \infty} = e^{-\rho \int (1 - e^{i\underset{\sim}{k} \cdot \underset{\sim}{E}(r)}) d^3r}$$

which with $\underset{\sim}{E}(r) = \frac{e\underset{\sim}{r}}{r^3}$ can be shown[1] to be the Fourier transform of the Holtsmark distribution function.

Now consider the pth term in the series argument of the exponential, $\frac{h^p}{p!} h_p(\underset{\sim}{k})$; this may be expressed as an integral, as indicated by Eq. (3.11), the value of which is determined by the properties of φ_i and s_p . The salient features of the s_p are: (1) They are different from zero only when the p particles are clustered; (2) The region of particle correlation is finite due to screening by the charged particles in the gas; (3) s_p goes to zero as T approaches infinity. Since the φ_i decrease rapidly as the distance from the field evaluation point is increased, the integral over all space is convergent. For finite values of k, $h_p(\underset{\sim}{k})$ is also finite. That the convergence of the integral is dependent on the factor is apparent since for large values of all the $\underset{\sim}{r}_i$ the s_p does not necessarily vanish since the particles may still be close together. One

would also expect that for finite k and large temperatures the successive terms in the exponential of (3.12) would be proportional to increasing powers of the inverse temperature. Then only a few terms in the expansion are necessary to get a good approximation for $F(\underset{\sim}{k})$ in the high-temperature region.

Eq. (3.12) is quite general and may be of interest, in the high-temperature limit, for a number of fields. The electric-field distribution follows immediately upon applying the inverse Fourier Transform to (3.12),

$$W(\underset{\sim}{E}) = \frac{1}{(2\pi)^3} \int e^{-i\underset{\sim}{k} \cdot \underset{\sim}{E}} F(\underset{\sim}{k})\, d^3k \qquad 3.13$$

C. <u>The High-Frequency and Low-Frequency Fields</u>

Before continuing in the calculation of the electric field distribution function, we will discuss the physical nature of the electric field contributions. Due to the differences in the time variation of their resultant fields, it is desirable to treat separately the electronic and ionic contributions to the total field. We follow the notation of Mozer and Baranger, referring to the field of the electron as the high-frequency component and that of the ions as the low-frequency component. That it is reasonable to consider the contributions separately is indicated not only by the differences in the time characteristics of the fields, but also by the fact that the collective fields of the electrons and ions are much different. In order to discuss these matters further, it is necessary to establish suitable time scales which are characteristic of the ionic and electronic motion. For this purpose, the concept of

relaxation times are introduced. If we consider a gaseous system of like particles which originally have an arbitrary velocity distribution, the time required for a Maxwellian velocity distribution to be established through collisions is referred to as the relaxation time.

It has been shown[53] that in a positive ion-electron gas, where the velocity distributions of both electrons and ions are initially arbitrary, the electrons will come to Maxwellian equilibrium much more rapidly than will the ions. The appropriate relaxation times which govern this approach to the Maxwellian distribution are taken as characteristic of the ionic and electronic motion.

Returning now to a consideration of the physical nature of the two field components, we realize that it is not correct to use a Coulomb field for the individual ions; such a procedure would completely neglect the ion-electron interaction. The low-frequency component contains a contribution from the electrons since the ion-electron interaction establishes a shielding electron cloud about each of the ions. Thus, the low-frequency component consists of a sum of all the separate shielded fields. The correct method for obtaining the low-frequency component is to calculate the time average of the electric field for a given ion configuration; the time over which the average is computed should be short compared to the ionic relaxation time, but long compared to the corresponding electron time. Since we are involved with a time-averaged component here, it is proper to use a Debye-Hückel shielded field for each ion.[1] Note that the shielding is due solely to electrons; ion-ion interactions are taken into account in the pair-correlation functions.

Because the ionic time of relaxation is much longer than that for electrons, an average of the high-frequency component of the micro-field over times the order of the ionic relaxation time, will vanish. Hence, it is reasonable to consider the high-frequency component as a gas of electrons imbedded in a uniform neutralizing background.

The above procedure is essentially that followed by those who describe plasma behavior by collective coordinates.[26] However, the arguments presented here are not intended to imply anything more than plausibility. The concept of low-frequency and high-frequency components can be derived more rigorously from the collective-coordinate approach.[26]

At this juncture the Mozer-Baranger approach resorts to the usual Debye-Hückel method to determine the shielded fields of the individual ions. The validity condition for this technique is that the volume of the electron cloud is large compared to the average volume per particle.[27] Thus, the ion field is found to be

$$\underset{\sim}{E}_i = \frac{e\underset{\sim}{r}_i}{r_i^3}\left(1 + \frac{r_i}{\lambda}\right) e^{-r_i/\lambda} \tag{3.14}$$

where λ = Debye length.

Consider now the two-body correlation function which will subsequently be used. For the high-frequency component, treated as a gas of electrons against a uniform neutralizing background, the potential of the mean force is given by:

$$w_2\left(\underset{\sim}{r}_1, \underset{\sim}{r}_2\right) = \frac{e^2}{r_{12}} e^{-\frac{r_{12}}{\lambda}} \tag{3.15a}$$

and the corresponding correlation function is:

$$V^2 P_2(\underset{\sim}{r}_1, \underset{\sim}{r}_2) = e^{-\beta w_2(\underset{\sim}{r}_1, \underset{\sim}{r}_2)} \tag{3.15b}$$

These expressions may be derived by the Debye-Huckel method, but for the purpose of this dissertation they are defined and derived from a different point of view in the next chapter, as are the following results for the low-frequency component:

$$w_2(\underset{\sim}{r}_1, \underset{\sim}{r}_2) = \frac{e^2}{r_{12}} e^{-\frac{r_{12}}{\lambda\sqrt{2}}} \tag{3.16a}$$

and

$$V^2 P(\underset{\sim}{r}_1, \underset{\sim}{r}_2) = e^{-\beta w_2(\underset{\sim}{r}_1, \underset{\sim}{r}_2)} \tag{3.16b}$$

It is seen from these equations that the only difference between the two-body correlation functions for the electron and ion cases is contained in the definition of the shielding length, λ or $\lambda/\sqrt{2}$.

D. <u>The Fourier Transform of the Field at a Neutral Point</u>

The following procedure will be considered in some detail and is applicable to either the high-or low-frequency case.

The neutral point at which the field is to be evaluated (the field evaluation point) is chosen to be the origin of the coordinate system. In this case the $s_1(\underset{\sim}{r}_i) = 1$ and the one-body term, $\rho h_1(k)$, is

$$\rho h_1(\underset{\sim}{k}) = \rho \int (e^{i\underset{\sim}{k} \cdot \underset{\sim}{E}_1} - 1)\, d^3 r_1 \tag{3.17}$$

Since $\underset{\sim}{E}_1 = \underset{\sim}{E}_1(r_1)$ we may set $k = \hat{i}_z k$ with no loss of generality, and Eq. (3.17) reduces to

$$\rho h_1(k) = -4\pi\rho \int_0^\infty (1 - j_o(kE_1))\, r_1^2\, dr_1 \tag{3.18}$$

where j_o is the zero-order spherical Bessel function[28], and E_1 is the magnitude of the single-particle field; a shielded field is used for the low-frequency case and a Coulomb field for the high-frequency case. In the latter instances (3.18) may be evaluated analytically, yielding

$$\rho h_1(k) = -\frac{4}{15}\rho(2\pi ek)^{3/2} \tag{3.19}$$

which depends only on the magnitude of k. Prior to writing a similar expression for the low-frequency case (L.F.) it is convenient to make the following definitions:

(a) A unit of length r_o is defined by

$$\frac{4}{15}(2\pi)^{3/2} r_o^3 \rho = 1$$

r_o is almost equal to the radius r_o', where

$$\frac{4\pi}{3} r_o'^3 \rho = 1$$

(b) The "normal" unit field strength E is defined by

$$E_o = \frac{e}{r_o^2}$$

(c) Two additional units are

$$\delta = \frac{|\underset{\sim}{E}|}{E_o}$$

and

$$x = |\underset{\sim}{k}| E_o$$

These units will be employed in the remainder of this chapter. Thus, (3.19) becomes:

H.F. $$\rho h_1 (k) = - x^{3/2} \qquad (3.19a)$$

The one-body term for the shielded field is given by

$$\rho h_1 (k) = - \frac{15}{(8\pi)1/2} \; x^{3/2} \int_o^\infty \left[1 + j_o(\xi)\right] Z^2 \, d\, Z \qquad (3.20)$$

where

$$\xi = Z^{-2} (1 + r_o/\lambda) \, x^{1/2} \, Z \exp\left[- (\frac{r_o}{\lambda}) \, x^{1/2} \, Z \right]$$

Z = r coordinate divided by $(ek)^{1/2}$

Further let us define

$$y \equiv \frac{r_o}{\lambda} x^{1/2} \qquad (3.21)$$

Hence, Eq. (3.20) may be written as

$$\rho h_1 (k) = - x^{3/2} \, \psi_1 (y)$$

This relation, which defines $\psi_1(y)$, must be evaluated numerically.

Now the two-body term, h_2, is found by letting $\mu_i = 2$ in Eq. (3.12). Thus, we have

$$\frac{\rho^2}{2!} h_2(\underset{\sim}{k}) = \frac{\rho^2}{2!} \int \cdots \int \varphi_1 \varphi_2 s_2(\underset{\sim}{r}_1, \underset{\sim}{r}_2) d^3r_1 d^3r_2 \qquad (3.22)$$

where from Eqs. (3.8) and (3.15)

$$s_2(\underset{\sim}{r}_1, \underset{\sim}{r}_2) = e^{-\beta w_2(\underset{\sim}{r}_1, \underset{\sim}{r}_2)} - 1 \qquad (3.23)$$

In the high-temperature limit one may linearize this expression:

$$s_2(\underset{\sim}{r}_1, \underset{\sim}{r}_2) \cong -\beta w_2(\underset{\sim}{r}_1, \underset{\sim}{r}_2) \ , \qquad (3.24)$$

which implies that

$$\frac{\rho^2}{2} h_2(\underset{\sim}{k}) \cong \frac{\rho^2}{2!\, kT} \int \int \varphi_1 \varphi_2 w_2(\underset{\sim}{r}_1, \underset{\sim}{r}_2) d^3r_1 d^3r_2 \ ; \qquad (3.25a)$$

or in dimensionless units,

$$\frac{\rho^2}{2} h_2(x) \cong x^{3/2} \psi_2(y) \qquad (3.25b)$$

Here $\psi_2(y)$ contains the two-body correction term. Thus, $\psi_1(y)$ and $\psi_2(y)$ refer to the appropriate one-body term and the two-body correction respectively. For the very high-temperature cases where the function $w_2(\underset{\sim}{r}_1, \underset{\sim}{r}_2)$ is given by the Debye-Hückel theory, it is possible

to evaluate this expression by expanding the various terms in the integrand in spherical harmonics. However we are not interested in this solution here. Attention will be confined to comments about the general character of Eq. (3.24) and its application to the calculation of microfield distribution function. It has been shown that the value of $h_2(\underset{\sim}{k})$ for the high-frequency component is much larger than the corresponding quantity for the low-frequency case; this is of course due to shielding effects.

The Fourier transform of the field distribution at a neutral point, Eq. (3.12), to the order of approximation used here can be expressed in dimensionless units as

$$F(x) = \exp\left[-x^{3/2}\left\{\psi_1(y) - \psi_2(y)\right\}\right] \tag{3.26}$$

An example of the two-body correction, $\psi_2(y)$ for the low-frequency case is shown together with the corresponding one-body term for comparison in Fig. 3. From this graphic illustration it is apparent that for values of x which do not make the exponential exceedingly small, and for values of r_o/λ from zero to one, $\psi_2(y)$ is indeed much smaller than $\psi_1(y)$. When the two-body correction is small compared to the one-body term, corrections from higher-order correlations should be negligible for the range of parameters in which we are interested.

E. Microfield Calculation

The Fourier transform of the field distribution, $F(\underset{\sim}{k})$, was shown to be independent of the k direction. This implies that the distribution function itself should also be independent of the k direction;

therefore, we define a function H(E) for the scalar quantity, E, or in dimensionless units $H(\delta)$:[49]

$$H(\delta) = 4\pi\delta^2 \; W \; (\underset{\sim}{\delta}) \tag{3.27}$$

If we now substitute the dimensionless form of Eq. (3.13) into Eq. (3.27) we find

$$H(\delta) = \frac{2\delta}{\pi} \int_0^\infty \sin(x\delta)\, F(x)\, x\, dx \tag{3.28}$$

This final expression has been evaluated numerically for both high- and low-frequency components at a neutral point. Results are presented in terms of the parameter r_o / λ,

$$\frac{r_o}{\lambda} = \left(\frac{15}{4}\right)^{1/3} \left(\frac{2q}{k}\right)^{1/2} \rho^{1/6} \; T^{-1/2} \tag{3.29}$$

where

q = electron charge

k = Boltzmann's constant

ρ = particle density

T = temperature in degrees Kelvin.

This quantity indicates the departure of the field distributions at finite temperatures from the infinite temperature or Holtsmark result, which is characterized by $r_o / \lambda = 0$.

Several graphs representing $H(\delta)$ for various cases and values of r_o / λ have been prepared. However, only the graph in Fig. 4 will be discussed. Here, for $r_o/\lambda = 0.6$, the low frequency $H(\delta)$ is shown for two cases: (1) only one-body terms included, (2) one- and two-body terms considered. Note that even though $\psi_2(y) << \psi_1(y)$, its inclusion has a pronounced effect on $H(\delta)$, the microfield distribution function; specifically, it raises the distribution maximum and shifts it markedly towards weaker fields. The conclusion is that even though $\psi_2(y)$ is a very small quantity, its nature strongly influences the form of $H(\delta)$. It will be shown in chapter V that the corrected $w_2^{L.F.}$ is considerably different from the Debye-Hückel result. Hence, this correction might be expected to alter W (E) or H (δ) considerably.

Figure 3

The One-ion Term Compared with the Two-ion Term for the Low-Frequency Component at a Neutral Point

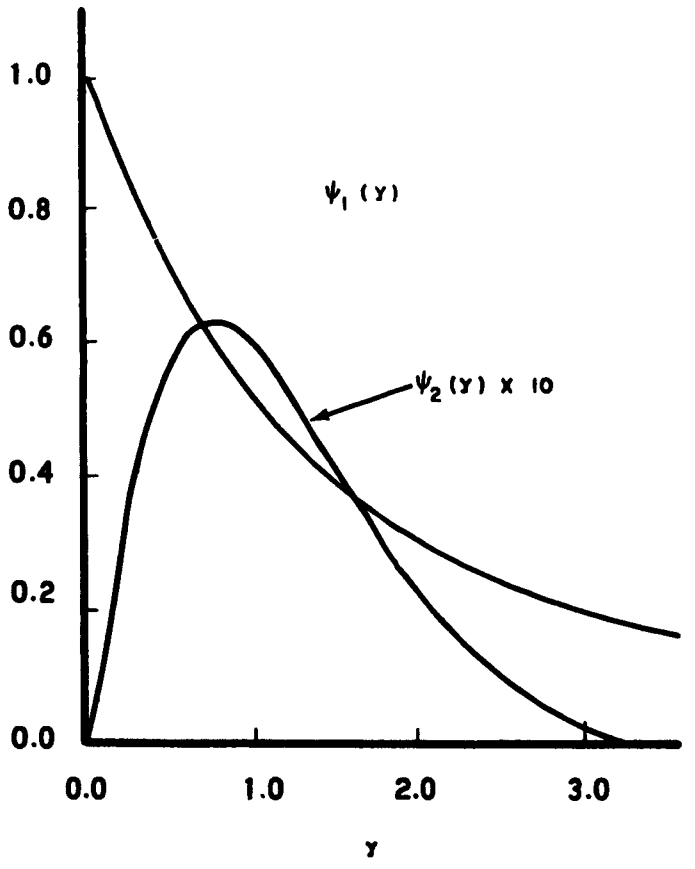

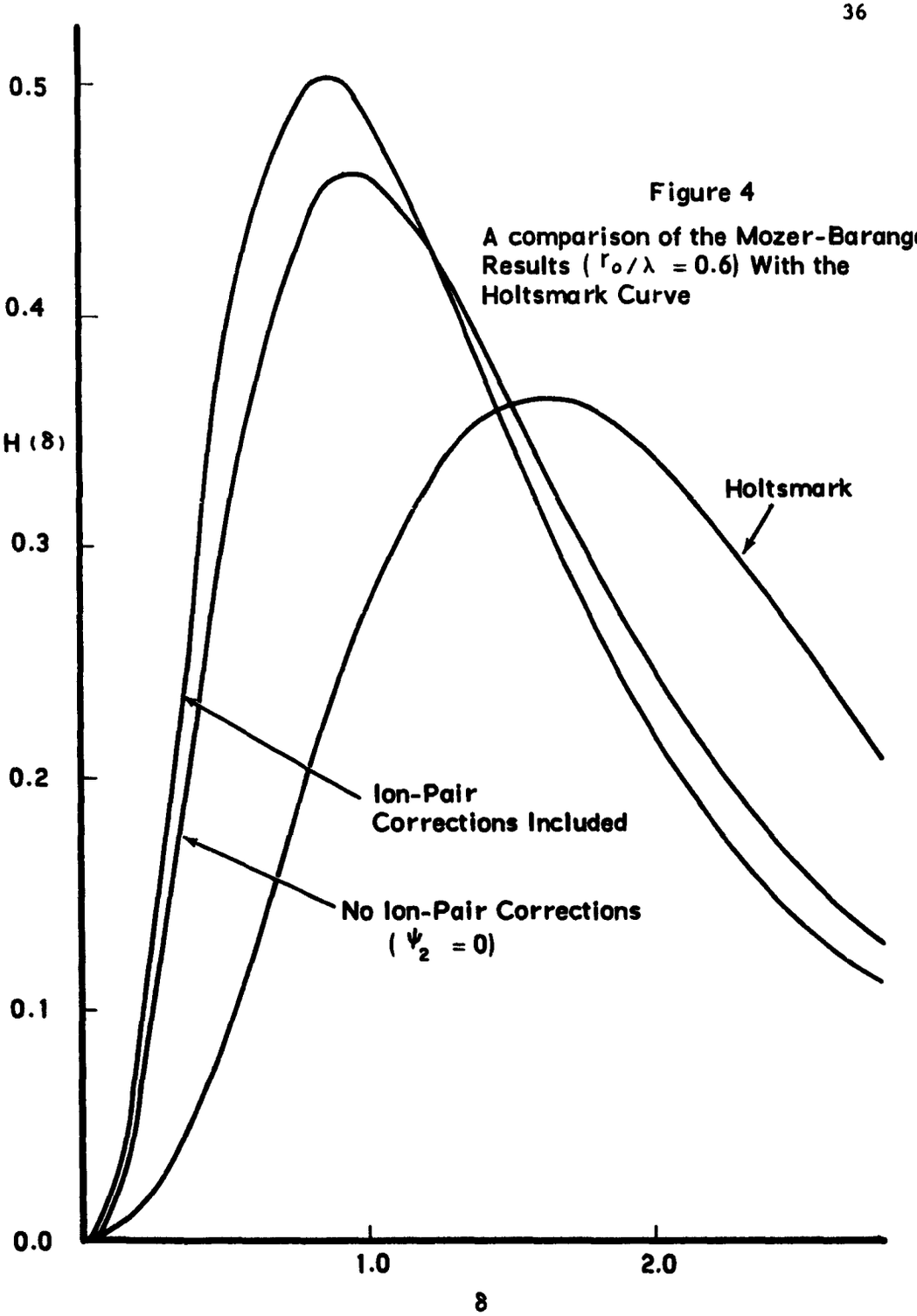

Figure 4

A comparison of the Mozer-Baranger Results ($r_o/\lambda = 0.6$) With the Holtsmark Curve

IV. CALCULATION OF PAIR-CORRELATION FUNCTIONS

A. Introduction

A large number of problems in statistical mechanics is concerned with calculation of correlation functions for systems with large numbers of particles. The method of cluster expansions[22], [23] has been most successful in this regard when applied to systems of particles with very short range interactions. Using this technique, one is able to derive infinite expansions in powers of the particle density, ρ, for the many-body correlation functions. If the density of the system is sufficiently low and if the particle interactions have short range these expansions converge rapidly; this is true when dealing with neutral molecules.

However, in the case of long-range potentials, of which the Coulomb interaction is the prime example, this cluster expansion approach is not applicable regardless of how dilute the system may be. Debye and Hückel proposed a method (1923) for treating very low density systems involving Coulomb interactions. Since this work, several authors[9][22][47] have developed techniques for use with systems of finite density which yield for the Debye-Hückel result as a first approximation and which, at least in principle, also offer higher-order correction terms. Generally, these improved methods express the correlation functions in terms of complicated integral equations.

The present chapter will essentially present the Salpeter approach to the problem of calculating correlation functions for a collection of particles which interact through long-range potentials.

The problem of how to regroup the terms of a cluster expansion so as to give meaningful results when applied to situations involving long range potentials, is considered in detail. In this development of the expansion approach it will be assumed that we are dealing with an equilibrium system of volume V which contains N particles of mass M; there exists a central interaction potential $U(r_{ij})$ acting between any pair (i, j) of particles. The theory is classical in nature and assumes only two-body interactions. In order that the classical assumption be correct, infinitely attractive potentials are forbidden.

B. Preliminary Statistical Mechanical Considerations

In this section, some general concepts from statistical mechanics, which will be necessary in the discussion of the Salpeter theory, are discussed. Of central importance in statistical mechanics is the partition function. It is defined as

$$Z = \frac{1}{h^{3N} N!} \int \cdots \int e^{-\frac{H}{kT}} \; d^3p_1 \cdots d^3p_N \; d^3r_1 \cdots d^3r_N \qquad (4.1)$$

where:

$$d^3p_i = d\,p_{xi}\; dp_{yi}\; dp_{zi}$$

$$d^3r_i = d\,x_i\; d\,y_i\; dz_i$$

$$H = \sum_{i=1}^{N} \frac{1}{2M} \left(p_{xi}^2 + p_{yi}^2 + p_{zi}^2\right) + U(\underset{\sim}{r}_1 \cdots \underset{\sim}{r}_N)$$

H is the Hamiltonian of the system.

U is the potential energy of the system.

$\underset{\sim}{p}_i$ = momentum of the ith particle.

$\underset{\sim}{r}_i$ = coordinate of the ith particle.

h = Planck's Constant

Note, also, that N and V are considered large; it is frequently convenient to have both V and N approach infinity in such a way that the density, $\rho = \frac{N}{V}$, remains constant.

Explicitly using the above H and carrying out the integration over the momentum, we have

$$Z = \frac{Q_N V^N}{N ! \Lambda^{3N}} \tag{4.2}$$

where

$$Q_N = V^{-N} \int \cdots \int e^{-u(\underset{\sim}{r}_1 \cdots \underset{\sim}{r}_N)} d^3 r_1 \cdots d^3 r_N$$

$$\Lambda = \frac{h}{(2\pi m kT)^{1/2}} ; \quad u(\underset{\sim}{r}_1 \cdots \underset{\sim}{r}_N) = \frac{1}{kT} U(\underset{\sim}{r}_1 \cdots \underset{\sim}{r}_N) \tag{4.3}$$

Now Q_N is referred to as the configuration integral. Making the assumption that the potential energy $u(\underset{\sim}{r}_1 \cdots \underset{\sim}{r}_N)$ is equal to the sum of pair potentials, we write

$$u(\underset{\sim}{r}_1 \cdots \underset{\sim}{r}_N) = \sum_{1 \le i < j \le N} u(r_{ij}) \tag{4.4}$$

$$= \sum_{1 \le i < j \le N} u_{ij}$$

Then

$$Q_N = V^{-N} \int \cdots \int e^{-\sum_{i<j} u_{ij}} d^3r_1 \cdots d^3r_N \qquad (4.5)$$

(1) Distribution and Correlation Functions[3]

It is now possible to define a distribution function. Suppose we observe a particular equilibrium configuration of N particles whose interaction potential is given by $u(\underset{\sim}{r}_1 \cdots \underset{\sim}{r}_N)$. The probability that particle 1 will be in d^3r_1, 2 in d^3r_2, and N in d^3r_N, is given by

$$P_N(\underset{\sim}{r}_1 \cdots \underset{\sim}{r}_N)dr_1 \cdots dr_N = V^{-N} Q_N^{-1} e^{-u(\underset{\sim}{r}_1 \cdots \underset{\sim}{r}_N)} d^3r_1 \cdots d^3r_N \qquad (4.6)$$

The probability $p_n(\underset{\sim}{r}_1 \cdots \underset{\sim}{r}_n)\, d^3r_1 \cdots d^3r_n$ that particle 1 will be in d^3r_1, 2 in d^3r_2, $\cdots$, n in d^3r_n regardless of the arrangement of the remaining N - n particles, is the sum of all probabilities (4.6) consistent with the specified (1 $\cdots$ n) configuration: i.e.,

$$p_n(\underset{\sim}{r}_1 \cdots \underset{\sim}{r}_n) = V^{-N} Q_N^{-1} \int \cdots \int e^{-u(\underset{\sim}{r}_1 \cdots \underset{\sim}{r}_N)} d^3r_{n+1} \cdots d^3r_N, \qquad (4.7)$$

subject to the normalization condition

$$\int \cdots \int p_n(\underset{\sim}{r}_1 \cdots \underset{\sim}{r}_n)\, d^3r_1 \cdots d^3r_n = 1 \quad . \qquad (4.8)$$

If we remove the restriction that particle 1 be in d^3r_1, 2 in d^3r_2, etc., and specify only that one particle be in each

element d^3r_i, the correct probability function to use is $\rho_n(\underset{\sim}{r}_1 \cdots \underset{\sim}{r}_n)$; it is related to $p_n\ (\underset{\sim}{r}_1 \cdots \underset{\sim}{r}_n)$ by

$$\rho_n\ (\underset{\sim}{r}_1 \cdots \underset{\sim}{r}_n) = \frac{N\ !}{(N-n)\ !}\ \ p_n\ (\underset{\sim}{r}_1 \cdots \underset{\sim}{r}_n) \tag{4.9}$$

where the factor $\frac{N\ !}{(N-n)\ !}$ gives the number of possible ways such an arrangement can be made. The normalization condition here is

$$\int \cdots \int \rho_n\ (\underset{\sim}{r}_1 \cdots \underset{\sim}{r}_n)\ \ d^3r_1 \cdots d^3r_n = \frac{N\ !}{(N-n)!} \tag{4.9a}$$

Now, since this dissertation is concerned with plasmas, let us consider the application of these distribution functions to gaseous, or more generally, fluid systems. As examples, we choose ρ_1 and ρ_2. From Eq. (4.9)

$$\rho_1\ (r_1) = N\ p_1\ (r_1) \tag{4.10}$$

$$= N\ Q_N^{-1}\ V^{-N} \int \cdots \int e^{-u(\underset{\sim}{r}_1 \cdots \underset{\sim}{r}_N)} d^3r_2 \cdots d^3r_N$$

$$\rho_2\ (\underset{\sim}{r}_1\ ,\ \underset{\sim}{r}_2) = N\ (N-1)\ p_1\ (\underset{\sim}{r}_1, \underset{\sim}{r}_2) \tag{4.11}$$

$$= N\ (N-1)\ Q_N^{-1}\ V^{-N} \int \cdots \int e^{-u(\underset{\sim}{r}_1 \cdots \underset{\sim}{r}_N)}\ d^3r_2 \cdots d^3r_N$$

The normalization condition, Eq. (4.9a), with n = 1 yields

$$\int \rho_1\ (\underset{\sim}{r}_1)\ d^3r_1 = \frac{N}{(N-1)!} = N \tag{4.12}$$

In a fluid all points $\underset{\sim}{r}_1$ are equivalent if we neglect the boundary layer; that is, $\rho_1 (\underset{\sim}{r}_1)$ is independent of $\underset{\sim}{r}_1$. Hence, from Eq.(4.12)

$$\rho_1 = \frac{N}{V}$$

$$= \rho, \text{ the particle density}$$

The two-particle distribution function for the fluid case is only a function of the distance between two points. This may be expressed as

$$\rho_2 (\underset{\sim}{r}_1 , \underset{\sim}{r}_2) = \rho_2 (\underset{\sim}{r}_{12}) .$$

Again, using Eq. (4.9a) we find,

$$\iint \rho_2 (\underset{\sim}{r}_1 , \underset{\sim}{r}_2) \, d^3 r_1 \, d^3 r_2 = \frac{N !}{(N - 2) !}$$

or

$$\int \rho_2 (r_{12}) \, d^3 r_{12} = \frac{(N - 1) N}{V}$$

An examination of Eq. (4.8) shows that if the distribution of particles is completely random,

$$p_n = V^{-n} \tag{4.13}$$

p_n and ρ_n are said to be "independent" if they satisfy the following relations:

$$p_n (\underset{\sim}{r}_1 \cdots \underset{\sim}{r}_n) = p_1 (\underset{\sim}{r}_1) \cdots p_1 (\underset{\sim}{r}_n)$$

$$\rho_n (\underset{\sim}{r}_1 \cdots \underset{\sim}{r}_n) = \rho_1 (\underset{\sim}{r}_1) \cdots \rho_1 (\underset{\sim}{r}_n) \tag{4.14}$$

If, however, the n probabilities, $P_1(\underset{\sim}{r}_i)$, are not "independent", it is possible to define a correlation function, g_n, which provides a measure of the deviation of p_n or ρ_n from the "independent" value. Considering only ρ_n, we can write

$$\rho_n(\underset{\sim}{r}_1 \cdots \underset{\sim}{r}_n) = \rho_1(\underset{\sim}{r}_1) \cdots \rho_1(\underset{\sim}{r}_n)\, g_n(\underset{\sim}{r}_1 \cdots \underset{\sim}{r}_n)$$

Returning to the fluid case, (4.15)

$$\rho_n(\underset{\sim}{r}_1 \cdots \underset{\sim}{r}_n) = \rho^n\, g_n(\underset{\sim}{r}_1 \cdots \underset{\sim}{r}_n)$$

From Eqs. (4.7), (4.9), and (4.15),

$$g_n(\underset{\sim}{r}_1 \cdots \underset{\sim}{r}_n) = \frac{V^{n-N}\, N!}{N^n\, (N-n)!}\, Q_N^{-1} \int \cdots \int e^{-u(\underset{\sim}{r}_1 \cdots \underset{\sim}{r}_n)}\, d^3r_{n+1} \cdots d^3r_N \qquad (4.16)$$

Since $$\frac{N!}{N^n(N-n)!} = 1 - \frac{n(n-1)}{2N} + \cdots$$

we can simplify Eq. (4.16) when terms of order $\frac{1}{N}$ are negligible. Thus, we write

$$g_n(\underset{\sim}{r}_1 \cdots \underset{\sim}{r}_n) = V^{n-N}\, Q_N^{-1} \int \cdots \int e^{-u(\underset{\sim}{r}_1 \cdots \underset{\sim}{r}_n)}\, d^3r_{n+1} \cdots d^3r_n \qquad (4.17)$$

$$= V^n\, p_n(\underset{\sim}{r}_1 \cdots \underset{\sim}{r}_n)$$

Closely connected with the correlation function is the potential of the mean force, defined by the equation[3]

$$g_n\ (\underset{\sim}{r}_1 \cdots \underset{\sim}{r}_n) = \exp\left\{ - w_n\ (\underset{\sim}{r}_1 \cdots \underset{\sim}{r}_n) \right\}, \qquad (4.17a)$$

where $w_n\ (\underset{\sim}{r}_1 \cdots \underset{\sim}{r}_n)$ is the potential of the mean force expressed in units of kT. Now recall that we are considering a system of N particles which interact through a potential $u(\underset{\sim}{r}_1 \cdots \underset{\sim}{r}_N)$, and that of these, only n have their coordinates $(\underset{\sim}{r}_1 \cdots \underset{\sim}{r}_n)$ specified. For such a system it can be shown[3] that the appropriate negative gradient of $w_n(\underset{\sim}{r}_1 \cdots \underset{\sim}{r}_n)$ gives the mean force acting on any one of the n particles, e.g., particle α. The mean potential differs from ordinary static potentials; in addition to the usual contribution from the n specified particles, it also has a contribution from the remaining (N - n). Hence, if we hold the n particles fixed and average over the other (N - n), we find that the mean force acting on particle α is

$$\overline{F}_\alpha = - \nabla_\alpha w_n \ .$$

(2) Cluster-Integral Expansions

In equation (4.5) there is a term in the integrand, $\exp\left[- \sum u_{ij} \right]$. Now introducing the function $f_{ij} = e^{-u_{ij}} - 1$, it is possible to write:

$$\begin{aligned} e^{- \sum u_{ij}} &= \prod e^{-u_{ij}} \\ &= \prod_{1 \le i < j \le N} (1 + f_{ij}) \\ &= 1 + \sum_{ij} f_{ij} + \sum_{ij} \sum_{kl} f_{ij}\, f_{kl} + \cdots \end{aligned} \qquad (4.18)$$

where (i, j) refers to any one of the possible N (N-1)/2 pairs. Each term in this expansion can be represented graphically by a diagram which corresponds to a factor f (r_{ij}); the total number of connecting lines in the graph equal the number of factors, f_{ij}, in the particular term under consideration. Note that for a finite-range potential f_{ij} goes to zero rapidly as the separation r_{ij} becomes large. To illustrate the cluster principle further, consider the various possibilities for a set of three particles:

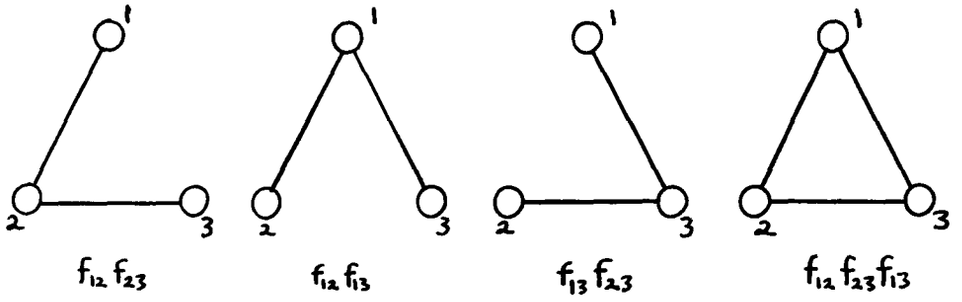

Figure 5 Clusters of Three Particles

The terms and corresponding diagrams comprising the expansions (4.18) can be classified and simplified systematically. For any diagram there is a definite number of points, ℓ, which are at least singly connected to particle 1. The portion of the diagram which involves the $\ell + 1$ connected points is designated a cluster; the remaining $N - (\ell + 1)$ points are not connected with the given $(\ell + 1)$ cluster, and may be arranged in an arbitrary manner.

Now consider the contribution to Q_N from a configuration involving an $(\ell + 1)$ particle cluster with the remaining $N - (\ell + 1)$ particles arbitrarily distributed.

The contribution from the (ℓ + 1) cluster is given by

$$I_{\ell+1} = V^{-(\ell+1)} \int d^3r_1 \cdots d^3r_{\ell+1} \prod f_{ij} \tag{4.19}$$

where the product of f_{ij} includes all such factors occurring in the diagram. $I_{\ell+1}$ multiplied by an integral over the remaining N - (ℓ+1) particles yields the contribution to Q_N from the above arrangement. The sum of all possible distributions of the N - (ℓ+1) particles, while holding the (ℓ + 1) fixed, gives a total contribution to Q_N of

$$I_{\ell+1} \; Q_{N-(\ell+1)}$$

where (4.20)

$$Q_{N-(\ell+1)} = V^{-N+(\ell+1)} \int \cdots \int d^3r_{\ell+2} \cdots d^3r_N \, e^{-\sum_{\ell+2}^{N} u_{ij}}$$

Multiplying by a factor $\frac{(N-1)!}{\ell![N-(\ell+1)]!}$ allows for the fact that any of the (N-1) particles can be used together with particle 1 in making up the (ℓ + 1) cluster. At this point, we define a cluster integral as

$$b_{\ell+1} = \frac{1}{(\ell+1)!V} \sum^{(\ell+1)} \int \cdots \int d^3r_1 \cdots d^3r \prod f_{ij} \tag{4.21}$$

where $\sum^{(\ell+1)}$ indicates summation over all possible single cluster diagrams which can be found from (ℓ + 1) given particles.

Many of these cluster integrals can be further simplified. Suppose that a cluster of (ℓ + 1) points may be disconnected by breaking

it at a single point, r_j. Then $b_{\ell+1}$ may be written as the product of two integrals, one corresponding to each of the two component clusters; the integration is carried out over relative coordinates $(r_i - r_s)$, r_s being considered fixed; in principle these two independent integrals will depend on the fixed position of r_s, relative to the volume boundaries. By requiring the interaction potential to be finite, and by having V go to infinity, this dependence is eliminated.

A cluster of k points, in addition to particle 1, which cannot be reduced by a single break is termed irreducible; irreducible cluster integrals β_k are given by

$$\beta_k = \frac{1}{k!} \int \cdots \int d^3r_2 \cdots d^3r_{k+1} \sum^{(k)} \prod f_{ij} \qquad (4.22)$$

where $\sum^{(k)}$ indicates summation over all possible irreducible cluster diagrams which can be formed with (k + 1) given particles. For k = 0 there is no connection between point 1 and any other point; other examples are

Irreducible Integral	Diagram
$\beta_1 = \int d^3r_2 \; f_{12}$	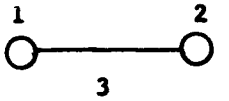
$\beta_2 = \frac{1}{2} \iint d^3r_2 \, d^3r_3 \, f_{12} \, f_{13} \, f_{23}$	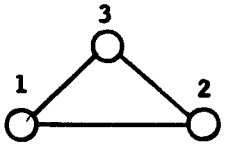

If it is possible to define other even more specialized classes of cluster integrals, but further comments about this will be deferred until the

discussion of the cluster expansion for the pair correlation function $g_2(\underset{\sim}{r}_1, \underset{\sim}{r}_2)$.

C. Cluster Expansion for the Pair Correlation Function

In this section a cluster expansion for the pair correlation function and for the potential of the mean force will be considered. In the limiting situation where both the particle number N and the system volume V approach infinity while the particle density $\rho = \frac{N}{V}$ remains constant, $g_2(\underset{\sim}{r}_1, \underset{\sim}{r}_2) = g_2(r_{12})$. From Eq. (4.16) it is seen that

$$g_2(r_{12}) = Q_N^{-1} V^{2-N} \int \cdots \int d^3r_3 \cdots d^3r_N \, e^{-\sum_{i<j}^{N} u_{ij}} \qquad (4.23)$$

The first step in the expansion development is the introduction of the "general 12 cluster"; this refers, by definition, to any diagram in which a number of, ℓ , particles are at least singly connected to either or both of the fixed points 1 and 2. See, for example, Fig. 6.

Figure 6 Two Examples of a General 12 Cluster

The corresponding cluster integrals are

$$b_o(r_{12}) = 1 + f_{12} = e^{-u_{12}} \qquad (4.24)$$

$$b_\ell(r_{12}) = \frac{1}{\ell!} \int \cdots \int d^3r_3 \cdots d^3r_{\ell+2} \sum^{(\ell)} \prod f_{ij}$$

where $\sum^{(\ell)}$ refers to summation over all possible cluster diagrams involving in addition to points 1 and 2, ℓ other points which will now be called field-points. The contribution to the integral in (4.7) from a diagram containing such a 12-cluster plus other disconnected diagrams, factors into a product of $b_\ell(r_{12})$ and the integrals involving the remaining $N - (\ell + 2)$ points.

Many of the general 12-cluster integrals can be reduced even further. We define a "general 12-irreducible cluster" with k given field-points as a diagram in which each of the k points lies on at least one continuous path which goes from point 1 to point 2 without passing any point more than once; such diagrams for k = 1, 2, and 3 are given in Fig. 7.

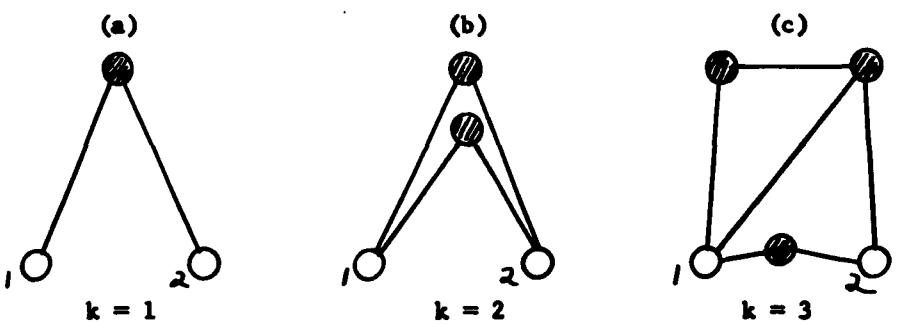

Figure 7 Examples of General 12-Irreducible Clusters

An even more restricted classification may be effected if the k field-points fall into two or more groups such that points in two different groups are interconnected only by paths which pass either through point 1 or 2. If this is the case, the diagram splits into independent

sub-diagrams by cutting at both point 1 and point 2. The corresponding general 12 cluster integral can then be written as a product of independent integrals, but where each factor is a function of r_{12}. A diagram in which no further cutting is possible is called "simple 12-irreducible"; see, for example, Fig. 8.

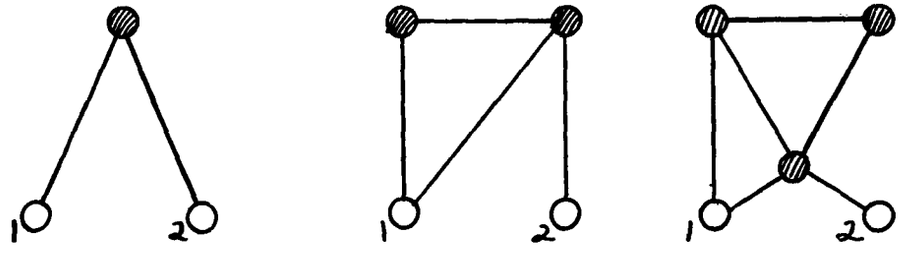

k = 1 k = 2 k = 3

Figure 8 Examples of Simple 12-Irreducible Clusters

"Simple 12-irreducible" cluster integrals, β_k, are defined as

$$\beta_k = \frac{1}{k!} \int \cdots \int d^3r_3 \cdots d^3r_{k+2} \sum^{(k)} \prod f_{ij} \qquad (4.25)$$

where $\sum^{(k)}$ denotes summation over all possible "simple 12-irreducible" cluster diagrams that can be obtained with the points 1, 2, and k given field-points. The factor f_{12} is not included in any of the products in this definition. For finite k and with both N and V approaching infinity, these integrals are functions only of the temperatures T and the relative distance r_{12}. Hence,

$$\beta_1 = \int d^3r_3 \; f_{13} \; f_{32} \qquad (4.26)$$

$$\beta_2 = \frac{1}{2!} \int\int d^3r_3\, d^3r_4\, f_{13}\, f_{34}\, f_{42} \left[2+4 \ldots f_{14} + f_{14}\, f_{23} \right]$$

where the numerical factor in brackets refer to the number of diagrams in which only the ordering of field-particles is different.

It is now possible to write down an expression for $g_2(r_{12})$; it requires only that one be able to find an expansion in powers of density, ρ, which has simple 1 2-irreducible cluster integrals as coefficients. Since further detail is concerned only with counting and collecting the various contributions, the result will be written down immediately,[2]

$$w_2(r_{12}) = u(r_{12}) - \sum_{k=1}^{\infty} \beta_k(r_{12}) \rho^k \tag{4.27}$$

$$g_2(r_{12}) = e^{-w_2(r_{12})} \tag{4.28}$$

These last two expressions are the desired result; their application to the case of the long range potentials is the subject of the next section.

D. The "Debye-Chain" Type of Expansion[2]

The irreducible cluster expansion in powers of the particle density, ρ, for the pair correlation function, $g_2(r_{12})$ and the corresponding potential of the mean force, $w_2(r_{12})$, was the subject of the previous section. It was indicated that it is possible to label each

irreducible cluster by the number of field-points k, and the number of connecting lines, ℓ , occurring in the given cluster. For a specific k value, the smallest possible value of ℓ is given by k + 1, and the largest by $\left[\frac{1}{2}(k+2)(k+1) - 1\right]$. In the usual expression for the irreducible cluster expansions, as shown in Eqs. (4.27) and (4.28), the diagrams are classified solely by k, all values of ℓ corresponding to this k being grouped together. When the particle system under consideration involves very short range interactions, i.e., neutral molecules, there is no trouble; in fact, this procedure proves quite satisfactory; when the range of the interaction r_M is much less than the average particle separation, $r_o \approx \rho^{-1/3}$. Thus, the condition for the "k only" grouping to be valid is that $\rho r_M^3 \ll 1$. Now consider such a short range potential, u_{ij}, which is large and repulsive at very small distances, slightly attractive at the potential minimum, and drops to zero rapidly for $r > r_M$. In this instance f_{ij} is or order unity inside the region r_M^3 , and drops to zero rapidly outside; the contributions to the cluster integrals β_k from an irreducible diagram with k field points and ℓ "lines" is then of order $(\rho r_M)^3$, regardless of the ℓ values; here we are excluding factors outside the integral, such as $\frac{1}{k!}$, etc.

An effective expansion parameter here is ρr_M^3 , and there is no need to regroup any terms according to ℓ values. In the event that the potential u_{ij} has a large (attractive) potential minimum, f_{ij} , becomes large and positive in the vicinity of this minimum. Thus, for a given value of k the largest contribution to β_k comes from diagrams

with fairly large ℓ values. Again, there is no reason to regroup the expansion terms. The situation is much different when the interaction potential is long range; here the "k only" arrangement is not correct.

In accordance with both classical mechanics and chapter three, a plasma model will now be adopted which involves only long-range, repulsive interactions; thus, consideration of attractive potentials in general, and infinitely attractive potentials in particular is avoided. This plasma is composed of singly charged ions and electrons, and involves interaction potentials (at the average distance of particle separation) that are small compared to thermal energy: i.e., $u_{ij}(r_{ij} \approx \rho^{-1/3}) \ll kT$; this condition implies a high-temperature, low-density system.

In this instance one hopes to find another small parameter in terms of which the cluster expansion may be constructed. The potential model will now be specified in three distinct regions:

(1) r less than some small distance, r_M; $u_{ij}(r)$ is large and positive.

(2) $r_M \leq r \leq \lambda$, where $\lambda \gg r_M$; $u_{ij}(r)$ is small, positive, and of order of magnitude ϵ, where ϵ is a constant much less than 1.

(3) $r \gg \lambda$; $u_{ij}(r)$ decreases more rapidly than r^{-3}.

It is further assumed that $(r_M/\lambda) \ll \epsilon \ll 1$. The function $f(r) = e^{-u(r)} - 1$ is then approximately equal to -1 in the region (1), of order ϵ in region (2), and is negligible in (3). Therefore, the total volume integral

(over all space) is of order $\epsilon \lambda^3$. Now only cases where the range of the potential is long compared to the average particle separation, i.e., $\lambda > \rho^{-1/3}$, or $\rho\lambda^3 > 1$ will be considered. Returning to the order of magnitude of the irreducible cluster integral, β_k, it is assumed that each integral contains k field-points with coordinates $\underset{\sim}{r}_i$ and ℓ "lines". The order of magnitude here is given by $\epsilon^{\ell}(\rho\lambda^3)^k$, or $\epsilon^{\ell-k}(\rho\epsilon\lambda^3)^k$. Although ϵ is by definition small, the quantity $\rho\epsilon\lambda^3$ may be large for sufficiently large λ. It is therefore useful to regroup the cluster expansion terms for $g_2(r_{12})$ according to the value of $\ell - k$; the summation is over k values for fixed $\ell - k$. This procedure is known as the cluster expansion in complexities.

Terms in Eq. (4.27) which correspond to values of $\ell - k = 1$, correspond to the "simple chain" diagrams illustrated below in Fig. 9. Recall that the term f_{12}, corresponding to k = 0, is missing from Eq. (4.27).

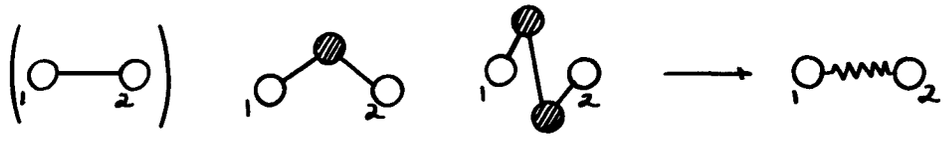

Figure 9 Clusters of the "Simple Debye Chain" Type

The sum, $\delta_1(r_{12})$, of the terms in Eq. (4.27) with $\ell - k = 1$ ($k \geq 1$) is given by

$$\delta_1(r_{12}) = \sum_{n=1}^{\infty} \rho^n \int \cdots \int d^3r_3 \cdots d^3r_{n+2}\, f(r_{13}) \cdots f(r_{n+2,\,2}) \qquad (4.29)$$

Setting $$\Gamma(r_{12}) = \delta_1 (r_{12}) + f (r_{12}) \tag{4.30}$$

it is observed that $\delta_1 (r_{12})$ is the Neumann-Liouville expansion for the function $\Gamma(r_{12})$; thus,

$$\Gamma(r_{12}) = f (r_{12}) + \rho \int d^3 r_3 \; f (r_{13}) \; \Gamma(r_{32}) \tag{4.31}$$

Taking Fourier transofrms, we find that the resulting equation may be solved by convolution techniques, yielding

$$\Gamma(k) = f (k) - \rho f(k) \; \Gamma(k)$$

or, (4.32)

$$\Gamma(k) = \frac{f (k)}{1 - \rho f (k)}$$

The solution of Eq. (4.31 or Eq. (4.32) represents in closed form, the summation of all diagrams with $\ell - k = 1$, for avbitrary k; convergence is now a question. It can be shown[2] that in the range $-\infty < \rho f(k) < +1$, Eq. (4.32) is justified.

If only the $\ell - k = 1$ terms are used in the expansion, we get as an approximation to the potential of the mean force, w_2:

$$w_2 (r_{12}) \cong u (r_{12}) - \delta_1 (r_{12})$$

$$= -\Gamma(r_{12}) + u(r_{12}) + f(r_{12}) \tag{4.33}$$

If u and f are of order $\epsilon \ll 1$ throughout the range of the potential then the error made in omitting terms with $\ell - k = 2$ is of order ϵ^2. Also note that

$$u + f = e^{-u} - 1 + u \simeq \frac{u^2}{2} + \cdots \tag{4.34}$$

and hence is, in the first approximation, of order ϵ^2. Using this first approximation f is replaced by, -u , in Eq. (4.31) giving

$$-w_2^{o}(r_{12}) = u(r_{12}) - \rho \int d^3 r_3 u(r_{13})\, w_2^{o}(r_{32}) \tag{4.35}$$

Applying the transform, convolution technique to this equation,

$$w_2^{o}(k) = \frac{-u(k)}{1 - \rho u(k)}$$

If

$$u(r_{12}) = \frac{\epsilon}{r_{12}} e^{-\alpha r_{12}} \tag{4.36}$$

where $\epsilon = \dfrac{q^2}{\lambda kT}$ and r_{12} is measured in units of the Debye length, λ . Then,

$$-u(k) = \frac{4\pi\epsilon}{k}\lambda^3 \int_0^{\infty} dr_{12}\, r_{12} \sin(kr_{12}) \cdot \frac{1}{r_{12}} e^{-\alpha r_{12}} \tag{4.37}$$

$$= \frac{4\pi\epsilon\lambda^3}{k^2 + \alpha^2}$$

Now it can be shown[52] that $4\pi\epsilon\rho = 1$. Thus, we have

$$w_2^{o}(k) = \frac{4\pi\epsilon\lambda^3}{k^2+\alpha^2+1} \tag{4.38}$$

$$w_2^{o}(r_{12}) = \frac{2\epsilon}{\pi r_{12}} \int_0^{\infty} dk\, k \sin(kr) \left[\frac{1}{k^2+\alpha^2+1}\right] \tag{4.39}$$

$$= \frac{2\epsilon}{\pi r_{12}} \left[\frac{\pi}{2} e^{-\sqrt{\alpha^2+1}\, r_{12}}\right]$$

For $\alpha = o$

$$w_2^{o}(r) = \frac{\epsilon}{r_{12}} e^{-r_{12}} \tag{4.40}$$

which is just the Debye-Huckel result. If $\alpha = 1$,

$$w_2^{o}(r) = \frac{\epsilon}{r_{12}} e^{-\sqrt{2}\, r_{12}} \tag{4.41}$$

Note that if u (r) is large and positive over even a small region of space, Eq. (4.35) becomes a very poor approximation to Eqs. (4.31) and (4.32). However, terms corresponding to $\hat{k} - k \geq 2$ which are neglected in equation (4.33) are still of order ϵ^2. This implies that for small ϵ they involve integrations to which this small region of space contributes little.

E. Higher-Order Terms

Thus far, only the $\ell - k = 1$ summation has been discussed. Terms for $\ell - k > 1$ may also be included as a sum of a finite number of integrals involving the $\Gamma(r)$ previously defined in Eq. (4.30).

Choose a typical irreducible cluster diagram occurring in Eq. (4.27) with arbitrary values of k and ℓ such as the diagram shown in Fig. 10-a.

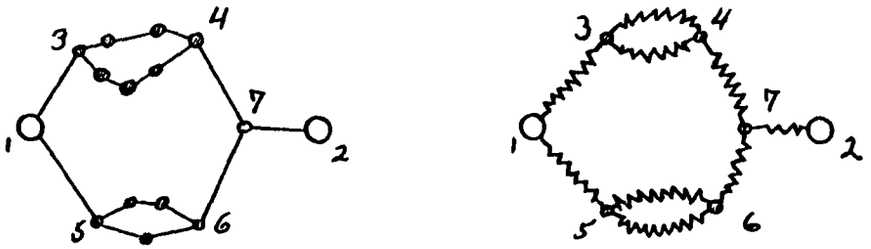

(a) (b)

Figure 10 An Example of a Simple 12-Irreducible Cluster, In Terms of "Wiggly Line" Diagrams.

In this diagram, each of the numbered points 3 to 7 are connected directly to at least three nearest neighbor points, whereas each of the unnumbered points are connected to only two neighbors. Fig. 10-b again shows this cluster diagram, but this time in terms of "wiggly lines", where each "wiggly" line represents a "simple chain" (Fig. 9). Now all diagrams which correspond to the same "wiggly line" diagram are considered together; although, the number of lines or links making up each "wiggly line" may be different in each case, the numerical value of $\ell - k$ is the same for all these diagrams.

In way of summary, the following "wiggly line" characteristics are listed:

1. Each field point lies on at least one continuous path between points 1 and 2.

2. Any pair of field points is connected by at least one continuous path which passes neither through point 1 nor 2.

3. Each field point is directly connected to at least three nearest neighbor points; if it were connected to only two nearest neighbors, it would be a mere link in the chain which contradicts the definition of a "wiggly line" diagram.

4. Any pair of points may be joined by more than one wiggly line.

Note that point 3. is in general not applicable to the usual irreducible cluster diagrams and that point 4. never applies to such diagrams.

Finally, an examination must be made into the nature of the wiggly line factors which occur in the integrands of the summed cluster integrals. Consider two points, (i, j) connected by a single wiggly line. This line, $_{i}O\sim\sim\sim\sim O_{j}$, represents the sum of the direct link, $f(r_{ij})$, plus all the simple chains with an arbitrary number of links (see Fig. 9). But, this sum is simply the function $\Gamma \equiv \mathcal{E} + f$ defined in Eq. (4.30). The general rule is that a single wiggly line between points i and j stand for a factor in the integrand; this may be compared with $f(r_{ij})$ for the ordinary cluster integrals. We next consider n parallel connections between i and j; here at most one of the n connections can stand for the direct link, $f(r_{ij})$. The factor in

the integrand is then the sum of two terms; the first term which does not contain the direct link, $f(r_{ij})$, consists of the product of n simple-chain factors, δ_1, and to account for the possible chain permutations, a factor $\frac{1}{n!}$ is included. The second term contains the direct f-link, and in addition, n - 1 simple chain factors. For each n-fold wiggly line connection between i and j, there is a factor in the integral of the form,

$$\Gamma_n(r_{ij}) = \frac{1}{n!}\ \delta_1^n(r_{ij}) + \frac{1}{(n-1)!}\ f(r_{ij})\ \delta^{n-1}(r_{ij}) \qquad (4.42)$$

Having thus obtained the function Γ or δ_1 from Eq. (4.31) or (4.32) we have an explicit integral for each wiggly line diagram. The value of $\ell - k$ is equal to the number of wiggly lines minus the number of field points; $\ell - k = 1$ implies a single such diagram while $\ell - k = 2$ gives rise to three graphs as seen in Fig. 11.

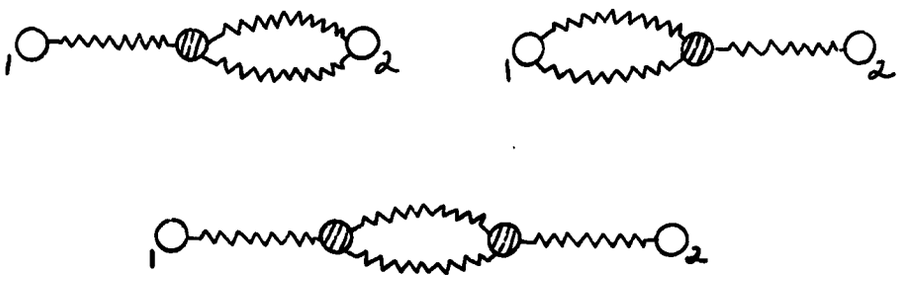

Figure 11 The Wiggly Line Diagrams For $\ell - k = 2$.

Returning to the potential of the mean force, and considering

terms up to and including $\ell - k = 2$, we find

$$u(r_{12}) - w_2(r_{12}) = \delta_1(r_{12}) + \left\{\rho\int d^3r_3\left[\Gamma^2(r_{13}) - f^2(r_{13})\right]\Gamma(r_{32})\right.$$

$$\left. + \frac{\rho^2}{2!}\iint d^3r_3\, d^3r_4\,\Gamma(r_{13})\left[\Gamma^2(r_{34}) - f^2(r_{34})\right]\Gamma(r_{42})\right. \tag{4.43}$$

This is the expression we have been seeking.

In order to make some comment about the magnitude of successive terms in this expansion, we again consider a repulsive potential of range λ, with u and f of order $\epsilon << 1$ ($r < \lambda$), but with $|\rho\epsilon\lambda^3| \geq 1$. From consideration of the Fourier transform it may be shown that $\rho|f(k)|$ is large for small k which in turn implies that $\Gamma(k) \approx 1$ for small k. Thus, it might be expected that $\Gamma(r)$ is comparable with $f(r) \sim \epsilon$ for small enough r, but decreases more rapidly than f (r) for $r >> \lambda$. $|\Gamma(k)|$ for small k is of order $\int d^3r\,\Gamma(r) \sim \epsilon\lambda^3$ and we therefore further expect that $(\rho\epsilon\lambda^3)$ will be of order unity. If this is the case, the order of magnitude of any term for any value of $\ell - k$ may be estimated to be

$$\epsilon^{\ell - k}(\rho\epsilon\lambda^3)^k \approx \epsilon^{\ell - k} \tag{4.44}$$

Hence, terms corresponding to large complexity — (l - k) = large — may be expected to contribute little to the cluster expansions.

V. CORRECTION TO THE DEBYE-HÜCKEL THEORY AND ITS APPLICATION

A. Introduction

In this chapter the theory developed in the preceding chapter will be used to derive an expression for the potential of the mean force, w_2, which is then applicable to either the Coulomb or shielded potential. Correction to the usual Debye-Hückel expression for w_2 will be given to second order in complexity. Furthermore, the results of these corrections will be scrutinized in light of the discussion in Chapters II and III.

Corrections of the nature proposed have previously been calculated by D. L. Bowers[52] for the case of the Coulomb potential; however, in his work he made the error first of using inaccurate tables, and secondly, of using an incorrect computer technique. Since his calculations and detailed data are not available in the open literautre, it is not possible to determine the exact importance of these errors. In view of this uncertaintly it was felt worthwhile to repeat the Coulomb calculation in addition to considering the shielded field case.

The expression for the potential of the mean force, w_2, will be evaluated using first only the $\ell - k = 1$ term and then including the $\ell - k = 2$ contribution. Thus, we must consider

$$w_2(r_{12}) = u(r_{12}) + f(r_{12}) - \Gamma(r_{12}) - X(r_{12}), \qquad (5.1)$$

where

$$u(r_{12}) = \frac{U(r_{12})}{kT}$$

$$f(r_{12}) = e^{-u(r_{12})} - 1$$

$$\Gamma(r_{12}) = f(r_{12}) + \rho \int d^3r_3 \; f(r_{13}) \Gamma(r_{32})$$

$$X(r_{12}) = \rho \int d^3r_3 \left[\Gamma^2(r_{13}) - f^2(r_{13})\right] \Gamma(r_{32})$$

$$+ \frac{\rho^2}{2!} \int\int d^3r_3\, d^3r_4\, \Gamma(r_{13}) \left[\Gamma^2(r_{34}) - f^2(r_{34})\right] \Gamma(r_{42})$$

Thus, Γ corresponds to the $\ell - k = 1$ contribution while X indicates the contribution of the $\ell - k = 2$ terms.

Now, consider that we have a potential of the form

$$u(r_{12}) = \frac{\epsilon}{r_{12}} e^{-\alpha r_{12}} \tag{5.2}$$

where

$r_{12} = \frac{R_{12}}{\lambda_D}$ = radial separation in units of λ_D

$\lambda_D = \left[\frac{kT}{4\pi q^2 \rho}\right]^{1/2}$ = Debye length

$\epsilon = \frac{q^2}{\lambda_D kT} = \left[4\pi\rho\lambda_D^3\right]^{-1}$

α = adjustable parameter , $0 \leq \alpha \leq 1$

Note that ϵ gives a measure of the strength of the interaction energy relative to the thermal energy.

As was shown in Chapter IV, in the event ϵ approaches zero, Γ

approaches Γ_c which is just the Debye-Hückel result. In the present notation,

$$\Gamma_o(r_{12}) = -\frac{\epsilon}{r_{12}} e^{-\sqrt{\alpha^2 + 1}\, r_{12}} \tag{5.3}$$

The values of ϵ which will be considered are $\epsilon = 0.1$ and 0.2. These are considered small values; from Eq. (4.54), it is known that the order of magnitude of the ratio of the $\ell - k = 2$ terms to those for which $\ell - k = 1$ will be ϵ, while the ratio of higher order terms to the $(\ell - k) = 1$ terms will be ϵ^2. Therefore, it is expected that the $\ell - k = 2$ terms will provide a satisfactory stopping point.

To simplify notation, we will set $r_{12} = r$ in the remainder of this chapter.

B. Evaluation of $\Gamma(r)$

From the theory of Fourier integrals we may write the following 3-dimensional transforms,

$$F(k) = \frac{4\pi}{k} \int_0^\infty dr\, r \sin(kr) F(r)$$

$$F(r) = \frac{1}{2\pi^2 r} \int_0^\infty dk\, k \sin(kr) F(k) \tag{5.4}$$

The Fourier transform $\Gamma(k)$ has been shown in Eq. (4.32) to be simply

$$\Gamma(k) = \frac{f(k)}{1 - \rho f(k)}$$

Since $f(r) = e^{-u(r)} - 1$ and $u(r) = \frac{\epsilon}{r} e^{-\alpha r}$ we may write the transform of f (r) as

$$f(k) = \frac{4\pi}{k} \int_0^\infty dr\, r \sin(kr) \left[e^{-\frac{\epsilon}{r} e^{-\alpha r}} - 1 \right] \qquad (5.5)$$

It is possible to effect an approximate solution of this integral by brute force techniques, but the solution for $\alpha \neq 0$ is so cumbersome that it is of little use. In the event that one is interested in the limiting case of $\alpha \longrightarrow 0$, the resulting solution may be expressed in terms of $\ker_2$ functions:[38]

$$\underset{\alpha=0}{f}(k) = -\frac{4\pi\epsilon}{k^2} \cdot 2 \ker_2(\eta)$$

where (5.6)

$$\eta = (4 \epsilon k)^{1/2}$$

If, however, it is desired to solve the expression for f (k), for arbitrary α, another method must be devised. An approach which avoids the difficulties mentioned before is as follows:

Let $\frac{\epsilon}{r} e^{-\alpha r} = R$. The, the expression $\left[e^{-R} - 1 \right]$ can be expressed in terms of Mellin transforms,

$$e^{-R} - 1 = \frac{1}{2\pi i} \int_{\sigma - i\infty}^{\sigma + i\infty} \Gamma(s)\, R^{-s}\, ds \qquad -1 < \sigma < 0 \qquad (5.7)$$

Inserting the correct form for R and substituting in Eq. (5.5), we find

$$f(k) = \frac{4\pi}{k} \int_0^{\infty} dr\, r \sin(kr) \cdot \frac{1}{2\pi i} \int_{\sigma - i\infty}^{\sigma + i\infty} \Gamma(s) \left[\frac{\epsilon}{r} e^{-\alpha r} \right]^{-s} ds$$

Simplifying and inverting the order of integration, we have

$$f(k) = \frac{4\pi}{k} \cdot \frac{1}{2\pi i} \int_{\sigma - i\infty}^{\sigma + i\infty} \Gamma(s) \epsilon^{-s} ds \int_0^{\infty} dr\, r^{s+1} \sin(kr)\, e^{\alpha s r} \qquad (5.8)$$

Now define:

$$t = r/\epsilon \Rightarrow r = \epsilon t$$

$$\alpha \epsilon = a \Rightarrow \alpha r = \alpha \epsilon t = at \qquad (5.9)$$

Using these definitions, we get

$$\left[\frac{\epsilon}{r} e^{-\alpha r} \right]^{-s} = t^s e^{ast}$$

$$r \sin(kr) dr = \epsilon^2 t \sin(k \epsilon t) dt$$

$$= \epsilon^2 t \sin(bt) dt \qquad b = \epsilon k$$

Thus,

$$f(k) = \frac{4\pi\epsilon^2}{k} \cdot \frac{1}{2\pi i} \int_{\sigma - i\infty}^{\sigma + i\infty} \Gamma(s) ds \int_0^{\infty} dt\, t^{s+1} \sin(bt) e^{ast} \qquad (5.10)$$

Now observe the integral

$$\int_0^\infty t^{s+1} \sin(bt)\, e^{ast}\, dt$$

Since the real part of s is negative, the equation may be solved[39]

$$\int_0^\infty t^{s+1} \sin(bt)\, e^{ast}\, dt = \Gamma(s+2)\left[(as)^2 + b^2\right]^{-\frac{s+2}{2}} \sin\left[(s+2)\tan^{-1}\frac{b}{-as}\right] \tag{5.11}$$

Substitution back into Eq. (5.8) yields

$$f(k) = \frac{4\pi\epsilon^2}{k} \cdot \frac{1}{2\pi i} \int_{\sigma-i\infty}^{\sigma+i\infty} \frac{\Gamma(s)\,\Gamma(s+2)\sin\left[(s+2)\tan^{-1}(-\frac{b}{as})\right]}{\left[(as)^2 + b^2\right]^{\frac{s+2}{2}}} ds \tag{5.12}$$

This integral may be solved by contour integration. We choose the contour as shown in Fig. 12.

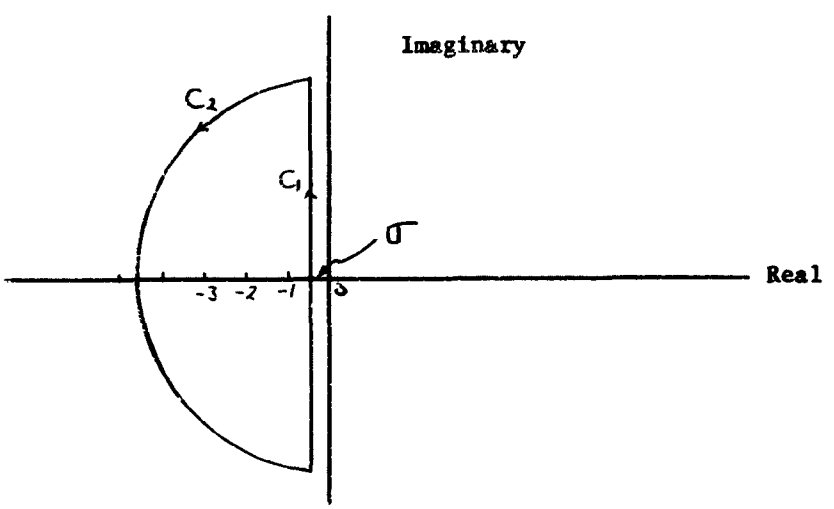

Figure 12

By Cauchy's residue theorem,

$$\int_{C_1} + \int_{C_2} = 2\pi i \sum \text{Residues} \tag{5.13}$$

It is shown in Appendix A that the contribution from $C_2 = 0$. Thus,

$$\int_{\sigma-i\infty}^{\sigma+i\infty} \frac{\Gamma(s)\,\Gamma(s+2)\,\sin\left[(s+2)\tan^{-1}\left(\frac{b}{-as}\right)\right]}{\left[(as)^2 + b^2\right]^{\frac{s+2}{2}}}\,ds = 2\pi i \sum \text{Residues} \tag{5.14}$$

Included inside the chosen contour are poles at all integer values on the negative real axis; these are due to singularities in the product of gamma functions. At $s = -1$ there is a single pole while for $s \geq -2$, the poles are all double. At $s = -1$ the residue is

$$R_{sp} = \text{Residue, single pole} = \left\{ \frac{(-1)^s\,\Gamma(s+2)\,\sin\left[(s+2)\tan^{-1}\left(\frac{b}{as}\right)\right]}{s!\quad\left[(as)^2 + b^2\right]^{\frac{s+2}{2}}} \right\}_{s=-1} \tag{5.15}$$

$$= -\frac{\sin\left[\tan^{-1}\frac{b}{a}\right]}{\left[a^2 + b^2\right]^{1/2}}$$

$$= -\frac{k}{\epsilon\left[\alpha^2 + k^2\right]}$$

For all other poles,

$$R_{DP} = \text{Residue, double pole, } = \left[\frac{d}{ds}\left\{(s+n)^2\,\Gamma(s)\,\Gamma(s+2)F(s)\right\}\right]_{s=-n} \tag{5.16}$$

where

$$F(s) = \frac{\sin\left[(s+2)\tan^{-1}\left(\frac{b}{-as}\right)\right]}{\left[(as)^2 + b^2\right]^{\frac{s+2}{2}}}$$

$$R_{DP} = \frac{1}{\Gamma(n-1)\Gamma(n+1)}\left[\left.\frac{dF(s)}{ds}\right|_{s=-n} - \frac{\Gamma'(n-1)}{\Gamma(n-1)} - \frac{\Gamma'(n+1)}{\Gamma(n+1)}\right] \quad (5.17)$$

Performing the operation $\left.\frac{d\,F\,(s)}{ds}\right|_{s=-n}$ yields,

$$\left.\frac{d\,F\,(s)}{d\,s}\right|_{s=-n} = \left[(an)^2 + b^2\right]^{\frac{n-2}{2}}\left\{\cos X\left[\frac{a\,b\,(n-2)}{(an)^2 + b^2} - \tan^{-1}\left(\frac{b}{an}\right)\right]\right.$$

$$\left. + \sin X\left[\ln\left((an)^2 + b^2\right)^{1/2} + \frac{a^2\,n\,(n-2)}{(an)^2 + b^2}\right]\right\}$$

where

$$X = \left[-(n-2)\tan^{-1}\left(\frac{b}{an}\right)\right]$$

Using this expression for $\left.\frac{d\,F\,(s)}{d\,s}\right|_{s=-n}$ in Eq. (5.17) gives for the residue at a double pole,

$$R_{DP} = \frac{\left[(an)^2 + b^2\right]^{\frac{n-2}{2}}}{\Gamma(n+1)\,\Gamma(n-1)}\left\{\cos X\left[\frac{a\,b\,(n-2)}{(an)^2 + b^2} - \tan^{-1}\left(\frac{b}{an}\right)\right]\right.$$

$$+ \sin X \left[\ln \left((an)^2 + b^2 \right)^{1/2} + \frac{a^2 n\,(n-2)}{(an)^2 + b^2} - \psi(n-1) - \psi(n+1) \right] \Bigg\} \quad (5.18)$$

where

$$\psi(n) = \frac{\Gamma'(n)}{\Gamma(n)}$$

Substituting Eq. (5.15) and (5.18) into Eq. (5.14) one finds that (5.12) becomes

$$f(k) = \frac{4\pi\epsilon^3}{b} \sum \text{Residues}$$

$$= \frac{4\pi\epsilon^3}{b} \left[- \frac{\sin\left[\tan^{-1}\left(\frac{b}{a}\right)\right]}{\left(a^2 + b^2\right)^{1/2}} + \sum_{n=2}^{\infty} \frac{\left[(an)^2 + b^2\right]^{\frac{n-2}{2}}}{\Gamma(n+1)/\Gamma(n-1)} \left\{ \right\} \right] \quad (5.19)$$

where

$$\left\{ \right\} = \left\{ \cos X \left[\frac{a\,b\,(n-2)}{(an)^2 + b^2} - \tan^{-1}\left(\frac{b}{an}\right) \right] \right.$$

$$\left. + \sin X \left[\ln\left((an)^2 + b^2\right)^{1/2} + \frac{a^2 n(n-2)}{(an)^2 + b^2} - \psi(n+1) - \psi(n-1) \right] \right\}$$

If $\alpha = 0$, and if the definitions in Eq. (5.9) are recalled, this general expression reduces to

$$f(k) = -\frac{4\pi\epsilon}{k^2} \left[1 + \sum_{n=2}^{\infty} \frac{(\epsilon k)^{n-1}}{\Gamma(n+1)/\Gamma(n-1)} \left\{ \frac{\pi}{2} \cos\left(\frac{n\pi}{2}\right) \right. \right. \quad (5.20)$$

$$\left. \left. + \sin\frac{n\pi}{2} \left[\ln(\epsilon k) - \Gamma(n+1) - \Gamma(n-1) \right] \right\} \right]$$

As is shown in Appendix B, this may be expressed in terms of modified Bessel functions:

$$f(k) = -\frac{4\pi\epsilon}{k^2} \cdot 2\,\mathrm{ker}_2\,\eta \qquad \eta = (4\epsilon k)^{1/2} \tag{5.21}$$

For $\alpha = 1$, corresponding to the Debye-Hückel shielded field, f (k) becomes

$$f(k) = -\frac{4\pi\epsilon}{k^2+1}\left[1 - \frac{k^2+1}{k}\sum_{n=2}^{\infty}\frac{\epsilon^{n-1}(n^2+k^2)^{\frac{n-2}{2}}}{\Gamma(n+1)\Gamma(n-1)}\left\{\right\}\right] \tag{5.22}$$

$$\left\{\right\} = \left\{\cos\left[(n-2)\tan^{-1}\left(\frac{k}{n}\right)\right]\left[\tan^{-1}\left(\frac{k}{n}\right) - \frac{k(n-2)}{n^2+k^2}\right]\right.$$

$$\left. + \sin\left[(n-2)\tan^{-1}\left(\frac{k}{n}\right)\right]\left[\ln\epsilon\,(n^2+k^2)^{1/2} + \frac{n(n-2)}{n^2+k^2} - \psi(n+1) - \psi(n-1)\right]\right\}$$

It is interesting to note that in Eqs. (5.20) and (5.22), the first term, due in each case, to the single order pole, corresponds to the Debye-Huckel result: if only this term is kept and the analysis carried on one finds that $\Gamma = \Gamma_o = -w_2^o$. The fact that all other terms arise from double poles is interpreted in the following manner: In the first approximation one takes only the first term in the expression. If higher order corrections are desired, it is necessary to include the entire summation over double poles and not just the first few such terms. Actual calculations confirm this last statement.

The above analytic expressions allow one to determine $\Gamma(k)$. However, it is not possible to get the inverse transform, $\Gamma(r)$, analytically.

Thus, the equation

$$\Gamma(r) = \frac{1}{2\pi^2 r} \int_0^\infty dk\, k \sin(kr) \left[\frac{f(k)}{1 - \rho f(k)} \right] \qquad (5.23)$$

is solved by computer techniques. Pertinent information about the computer approach is contained in Appendix D. It should be mentioned here, however, that in both instances for which numerical work was done, $\alpha = 0, 1$, the needed values of f (k) were generated by the machine from Eqs. (5.20) and (5.22) and are not tabular values. The above integration was performed for $\epsilon = 0.1, 0.2$ for both $\alpha = 0$ and $\alpha = 1$; the results are listed in Table I. Once $\Gamma(r)$ is known, it is immediately possible to find expressions for $w_2(r)$ and $g_2(r)$:

$$w_2(r) = u(r) + f(r) - \Gamma(r)$$

$$g_2(r) = e^{-w_2(r)}$$

The expressions found for $w_2(r)$ by this method are compared graphically with the corresponding Debye-Hückel results, $\Gamma_o(r) = w_2^o(r)$, in Figs. 13, 14, 15, and 16. It should be pointed out here that g_n can be related to the function s_n discussed in Chapter III[50]; specifically, setting n = 2, we find for a fluid system that

$$g_2(r) = 1 + s_2(r)$$

It is interesting to note that the corrected curve for $w_2 \left\{ \epsilon = 0.1, \alpha = 1 \right\}$ lies just above the Debye-Hückel curve, while

the result for w_2 $\{\epsilon = 0.1, \alpha = 1\}$ lies considerably below the corresponding Debye-Hückel curve. This implies that in the first instance the Debye-Hückel approximation overestimates the shielding, while in the second case, it underestimates the shielding. That such a result is at least possible may be seen by considering the graphs of f (k) for various values of ϵ as shown in Fig. 17. The Debye-Hückel result corresponds to $\epsilon = 0$, which fact implies that it is valid only in the infinite temperature limit, $T \longrightarrow \infty$. Now observe that as the magnitude of ϵ increases, the slope of the curve for smaller values of k increases noticeably, while the positive region of the curve becomes much larger and shifts toward the smaller k values. From actual computer runs, it is known that k values above $\sim$ 150 make negligible contributions to the integral expression for $\Gamma(r)$. As ϵ is increased, the curves for f (k) change as indicated above, but the positive portion of the curve does not become important until $\epsilon > 0.1$; the change in the curve which is important below $\epsilon \approx 0.1$ is the alteration of slope. This importance is apparent when one realizes that this function is multiplied by sin (kr) in the integrand. Thus, the slope change in the region below $\epsilon = 0.1$ is the primary cause of deviation from the Debye-Hückel curve. When the positive segment of the f (k) curve becomes appreciable, in the range of significant k values, this feature of the curve becomes the more important factor, and the corrected expression for $w_2(r)$ lies below its Debye-Hückel counterpart. This brief discussion is designed only to indicate that such an ϵ dependent shift is plausible.

TABLE I

$\Gamma(r)$ vs. r

$\alpha = 0$

$\epsilon = 0.1$		$\epsilon = 0.2$	
r	$\Gamma(r)$	r	$\Gamma(r)$
0.0	-1.33390	0.0	-0.82915
0.1	-0.83742	0.1	-0.68575
0.5	-0.10685	0.5	-0.16869
1.0	-0.03620	1.0	-0.04958
1.5	-0.01523	1.5	-0.01857
2.0	-0.00705	2.0	-0.00681
3.0	-0.00177	3.0	-0.00125

$\alpha = 1.0$

$\epsilon = 0.1$		$\epsilon = 0.2$	
r	$\Gamma(r)$	r	$\Gamma(r)$
0.0	-0.99404	0.0	-0.91017
0.1	-0.51042	0.1	-0.62486
0.5	-0.09401	0.5	-0.15745
1.0	-0.02454	1.0	-0.03720
1.5	-0.00853	1.5	-0.01233
2.0	-0.00304	2.0	-0.00377
3.0	-0.00049	3.0	-0.00040

Constants employed in these calculations were:

$\pi = 3.14159265$

γ = Euler's Constant = .577215665

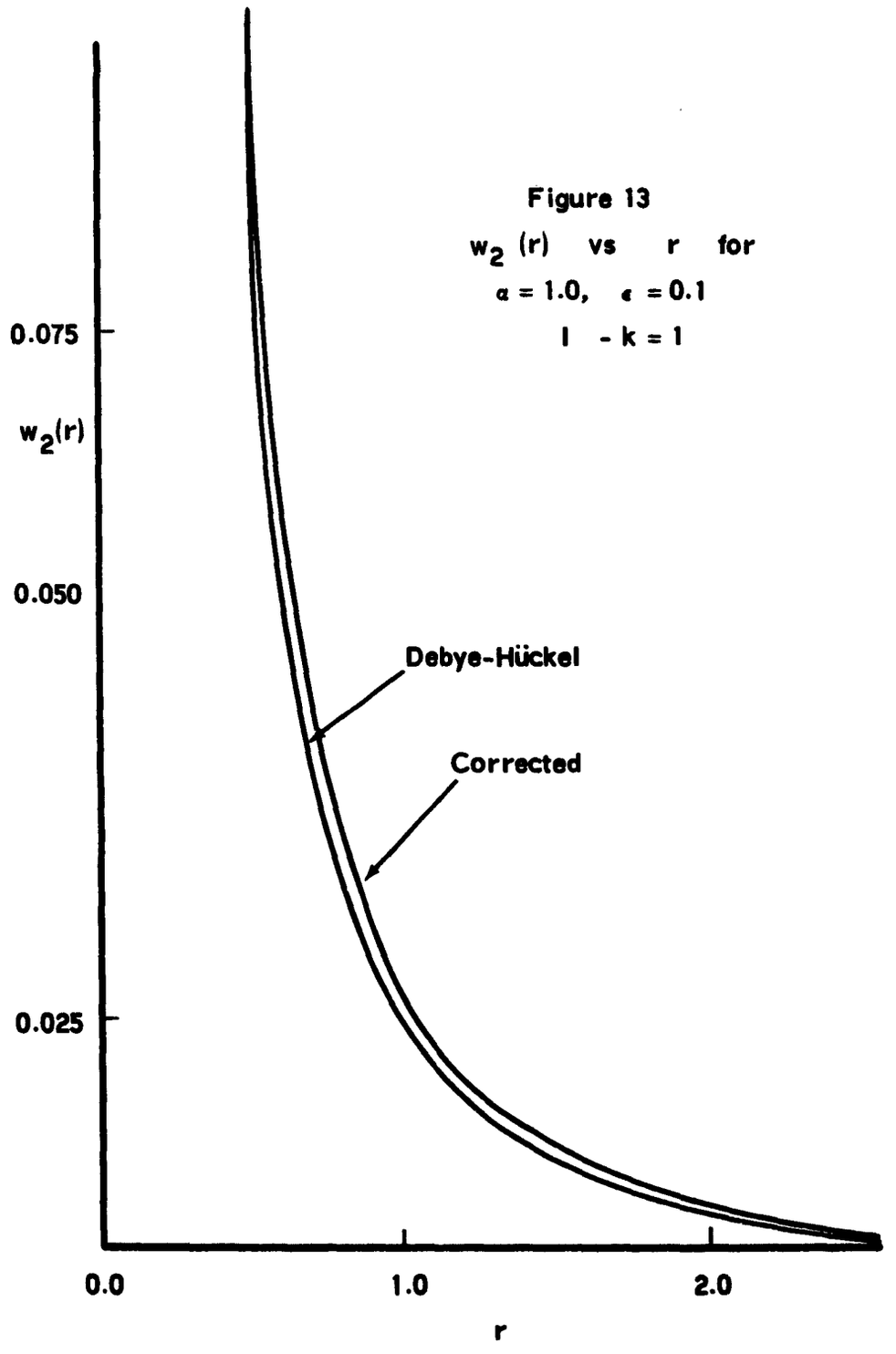

Figure 13
w_2 (r) vs r for
$\alpha = 1.0, \quad \epsilon = 0.1$
$I - k = 1$

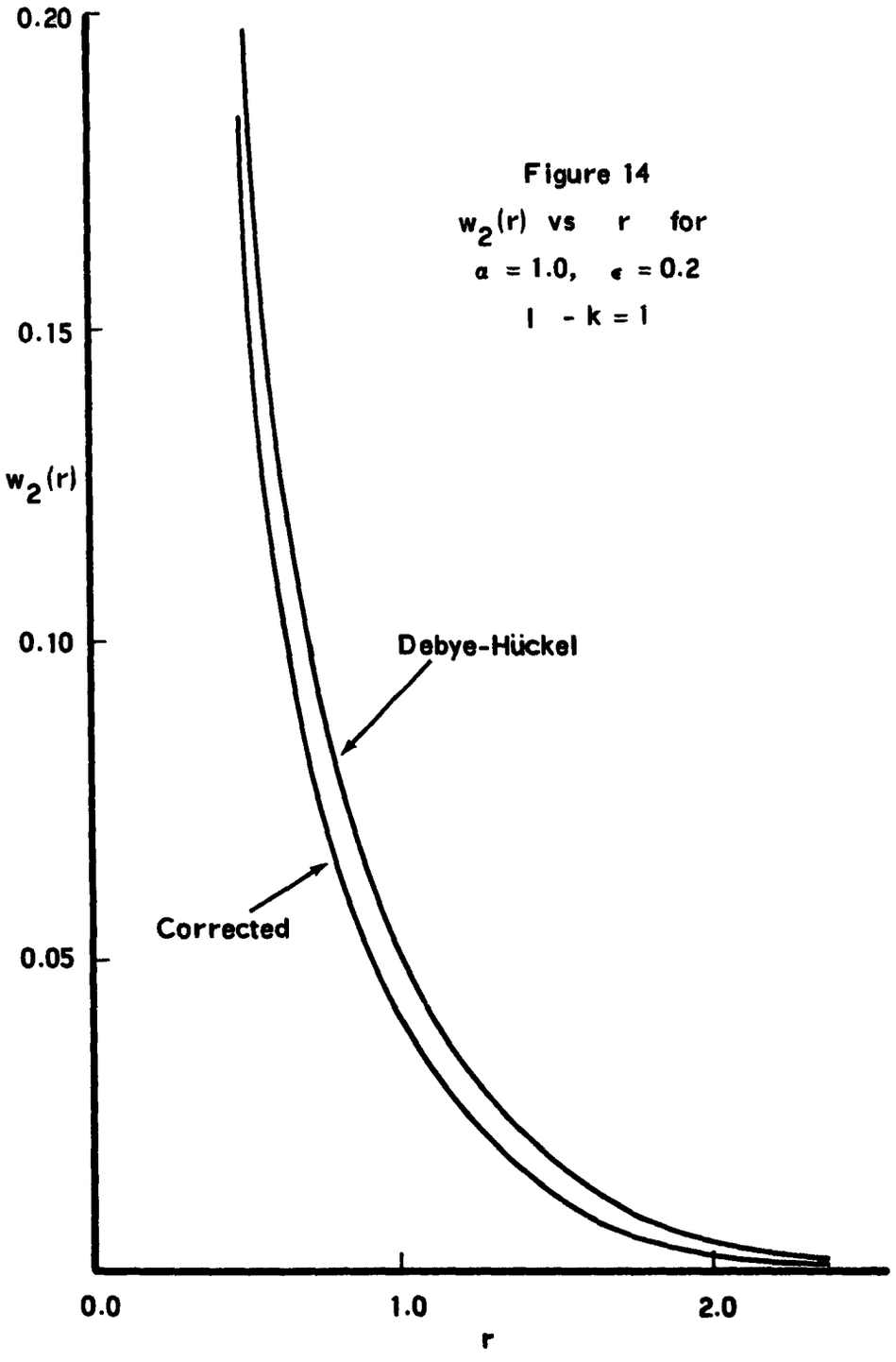

Figure 14
$w_2(r)$ vs r for
$\alpha = 1.0$, $\epsilon = 0.2$
$1 - k = 1$

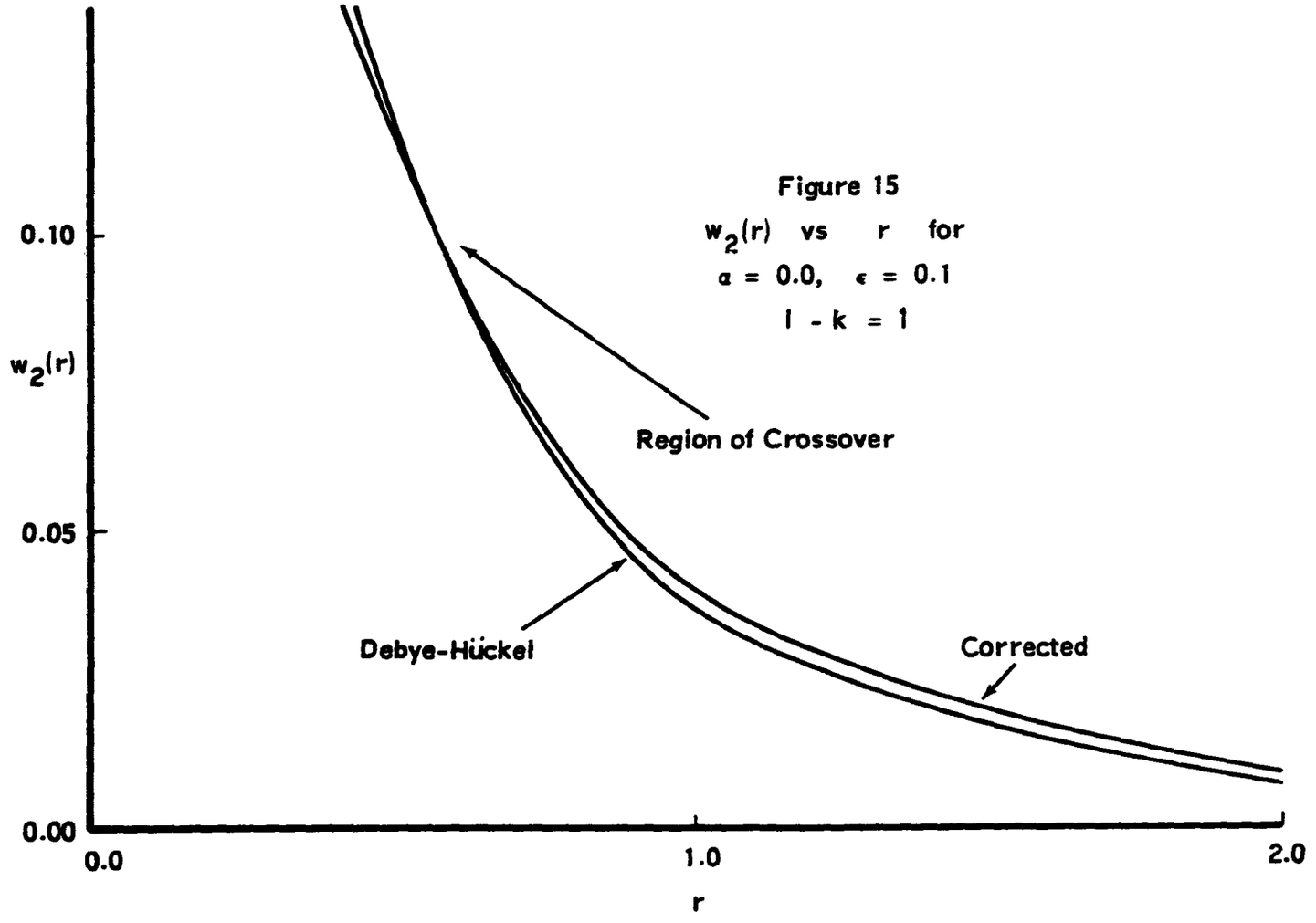

Figure 15
$w_2(r)$ vs r for
$\alpha = 0.0, \quad \epsilon = 0.1$
$l - k = 1$

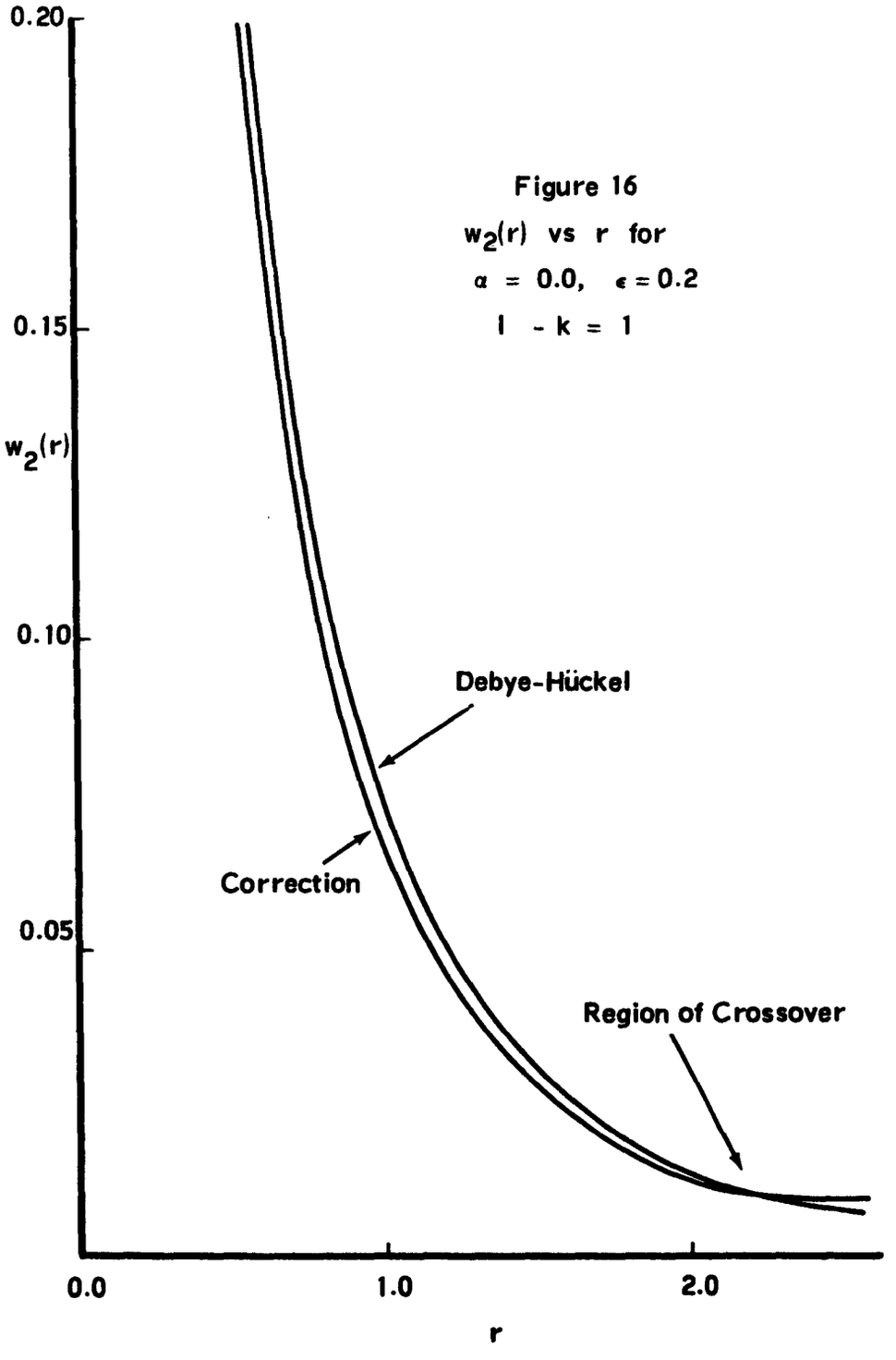

Figure 16
$w_2(r)$ vs r for
$\alpha = 0.0, \quad \epsilon = 0.2$
$l - k = 1$

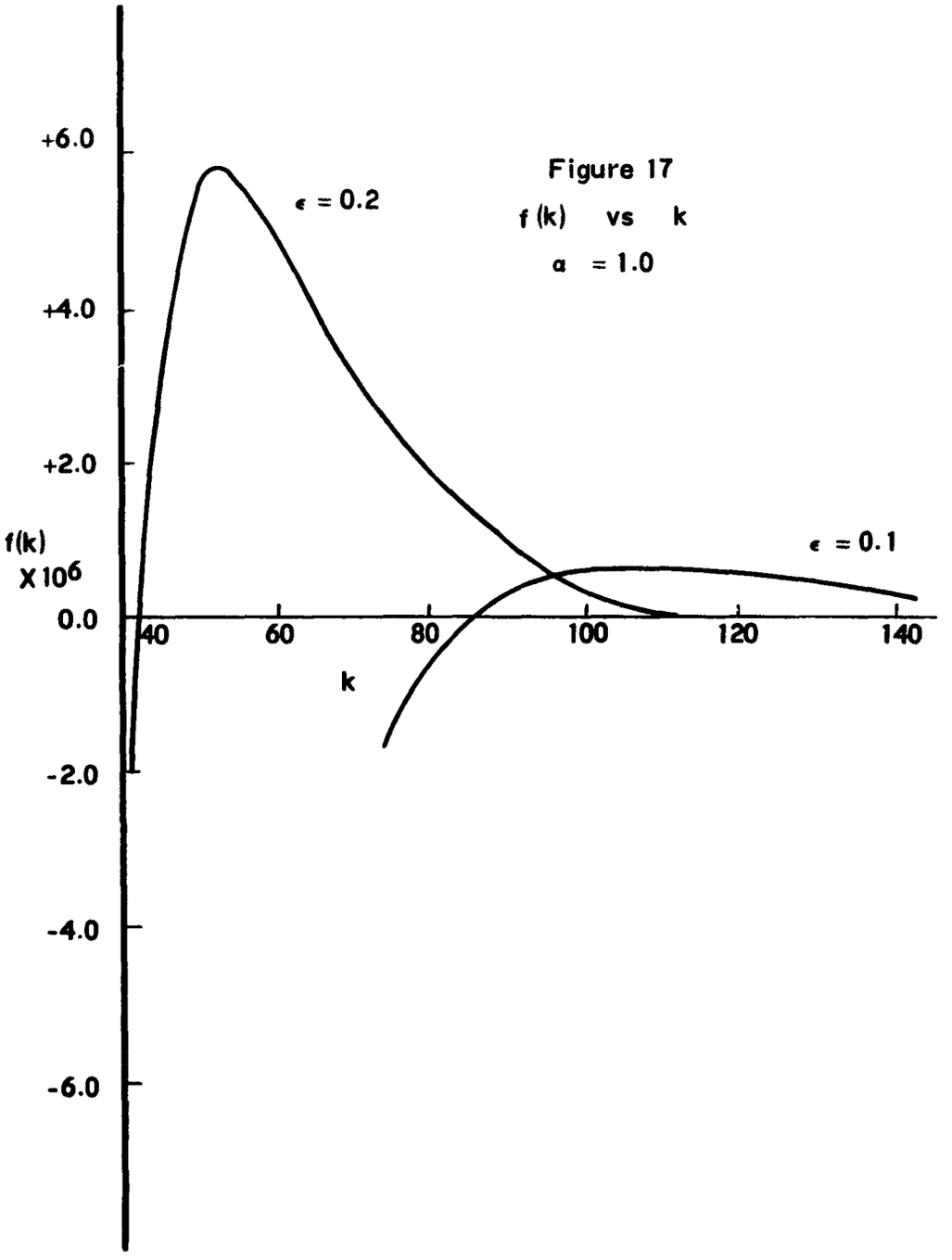

Figure 17
f (k) vs k
α = 1.0

For the cases $\alpha = 0$, $\epsilon = 0.1, 0.2$, the corrected $w_2(r)$ curves lie below the corresponding Debye-Hückel graphs until r approaches unity; in this region the corrected curves cross the approximate curves and remain above as r is increased. The $w_2(r)$ curve, for $\epsilon = 0.2$, deviates more from the Debye-Hückel result than does the $\epsilon = 0.1$ figure; furthermore, the crossing point in this case occurs for larger r values than is the case with $\epsilon = 0.1$. See Figs. 15 and 16. This implies that for $r < 1$ the Debye-Hückel approximation overestimates the shielding, while for $r > 1$ it underestimates it.

Now consider the contribution of the $\ell - k = 2$ term which are contained in X (r). From the preceding chapter, we use Eq. (4. 3).

$$X(r) = \rho \int d^3 r_3 \, \Gamma(r_{13}) \left[\Gamma^2(r_{32}) - f^2(r_{32}) \right]$$

$$+ \frac{\rho^2}{2} \int\int d^3 r_3 \, d^3 r_4 \, \Gamma(r_{13}) \left[\Gamma^2(r_{34}) - f^2(r_{34}) \right] \Gamma(r_{42})$$

Also, from arguments presented in the previous chapter, it is expected that the magnitude of this term will be of order ϵ^2. Now, since the expressions for $\Gamma(r)$ derived for $\ell - k = 1$ do not vary greatly from the Debye-Hückel results, X (r) will be evaluated setting $\Gamma(r) \cong \Gamma_o(r)$; this implies that X (r) is calculated to first order in ϵ. With this substitution, X (r) may be evaluated analytically; this calculation for arbitrary α is shown in detail in Appendix C. The final expression

is

$$X(r) = \frac{\epsilon^2}{8(\alpha^2+1)\,r}\left\{e^{-\sqrt{\alpha^2+1}\,r}\left[\frac{2\sqrt{\alpha^2+1}-2\alpha}{6\alpha\sqrt{\alpha^2+1}+3\alpha^2+3}\right.\right.$$

$$-\left[r-\frac{4\alpha^2+3}{\sqrt{\alpha^2+1}}\right]\left[\ln\left(\frac{1}{3}\cdot\frac{2\alpha-\sqrt{\alpha^2+1}}{2\alpha+\sqrt{\alpha^2+1}}\right)+E_{-}(\sqrt{\alpha^2+1}\,r)-E_{-}((2\alpha-\sqrt{\alpha^2+1})r)\right]$$

$$\left.-\frac{1}{2\alpha-\sqrt{\alpha^2+1}}\left(e^{-(2\alpha-\sqrt{\alpha^2+1})r}-1\right)+\frac{1}{\sqrt{\alpha^2+1}}\left(e^{-\sqrt{\alpha^2+1}\,r}-1\right)\right] \qquad (5.24)$$

$$-e^{+\sqrt{\alpha^2+1}\,r}\left[\left(r+\frac{4\alpha^2+3}{\sqrt{\alpha^2+1}}\right)\left(E_{-}(3\sqrt{\alpha^2+1}\,r)-E_{-}(2\alpha+\sqrt{\alpha^2+1})r\right)\right.$$

$$\left.\left.+\frac{1}{2\alpha+\sqrt{\alpha^2+1}}e^{-(2\alpha+\sqrt{\alpha^2+1})r}-\frac{1}{3\sqrt{\alpha^2+1}}e^{-3\sqrt{\alpha^2+1}\,r}\right]\right\}$$

For $\alpha = 0$ this reduces to:

$$X(r) = \frac{\epsilon^2}{8\,r}\left\{e^{-r}\left[\frac{4}{3}\,(e^{-r}-1)-(r-3)(E_1(r)-E_{-}(r)-\ln 3)\right]\right. \qquad (5.25)$$

$$\left.-e^{+r}\left[(r+3)(E_{-}(r)-E_{-}(3r))\right]\right\}$$

where

$$E_{-}(r) = \int_{+r}^{\infty}\frac{e^{-x}}{x}\,dx \quad ; \quad E_1(r) = \int_{-r}^{\infty}\frac{e^{-x}}{x}\,dx$$

For $\alpha = 1$, the expression (5.24) becomes

$$X(r) = \frac{\epsilon^2}{16}\left\{ e^{-\sqrt{2}r}\left[\frac{\sqrt{2}-1}{3\sqrt{2}+3} - \left(r - \frac{7\sqrt{2}}{2}\right)\left[\ln\frac{1}{3}\cdot\frac{2+\sqrt{2}}{2-\sqrt{2}} + E_{-}(\sqrt{2}r) - E_{-}\left((2-\sqrt{2})r\right)\right]\right.\right.$$

$$\left. - \frac{1}{2-\sqrt{2}}\left(e^{-(2-\sqrt{2})r} - 1\right) + \frac{1}{\sqrt{2}}\left(e^{-\sqrt{2}r} - 1\right)\right] \qquad (5.26)$$

$$- e^{+\sqrt{2}r}\left[\left(r + \frac{7\sqrt{2}}{2}\right)\left(E_{-}(3\sqrt{2}r) - E_{-}\left((2+\sqrt{2})r\right)\right)\right.$$

$$\left.\left. + \frac{1}{2+\sqrt{2}} e^{-(2+\sqrt{2})r} - \frac{1}{3\sqrt{2}} e^{-3\sqrt{2}r}\right]\right\}$$

These functions are shown graphically for both values of α in Figs. 18, 19 and 20, 21. Note that the contribution of the $\ell - k = 2$ terms is much less than that from the corresponding $\ell = k = 1$ expression; this is especially true in the shielded field case.

In the next chapter further implications of the results disclosed in the present chapter will be discussed.

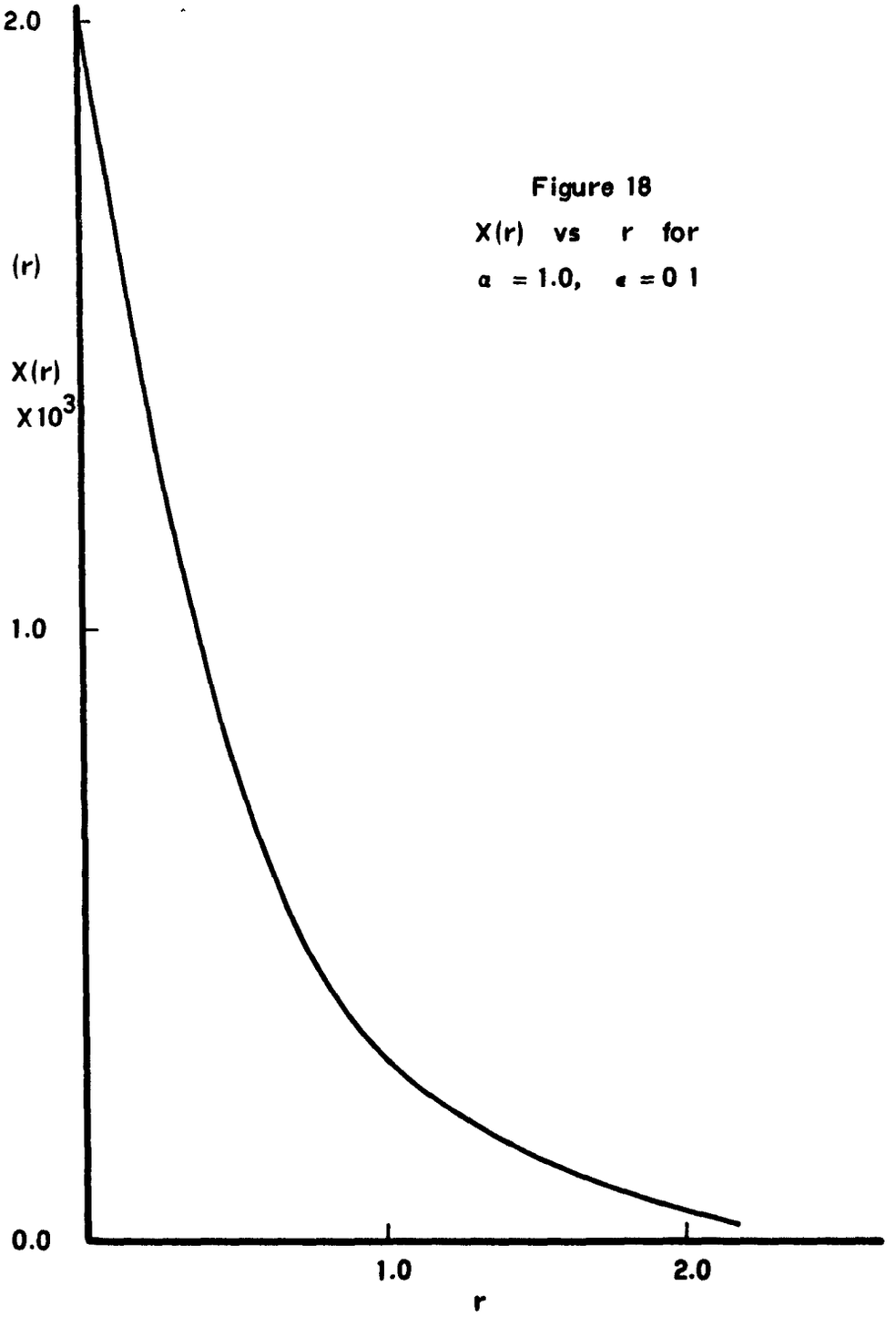

Figure 18
X(r) vs r for
$\alpha = 1.0, \quad \epsilon = 0.1$

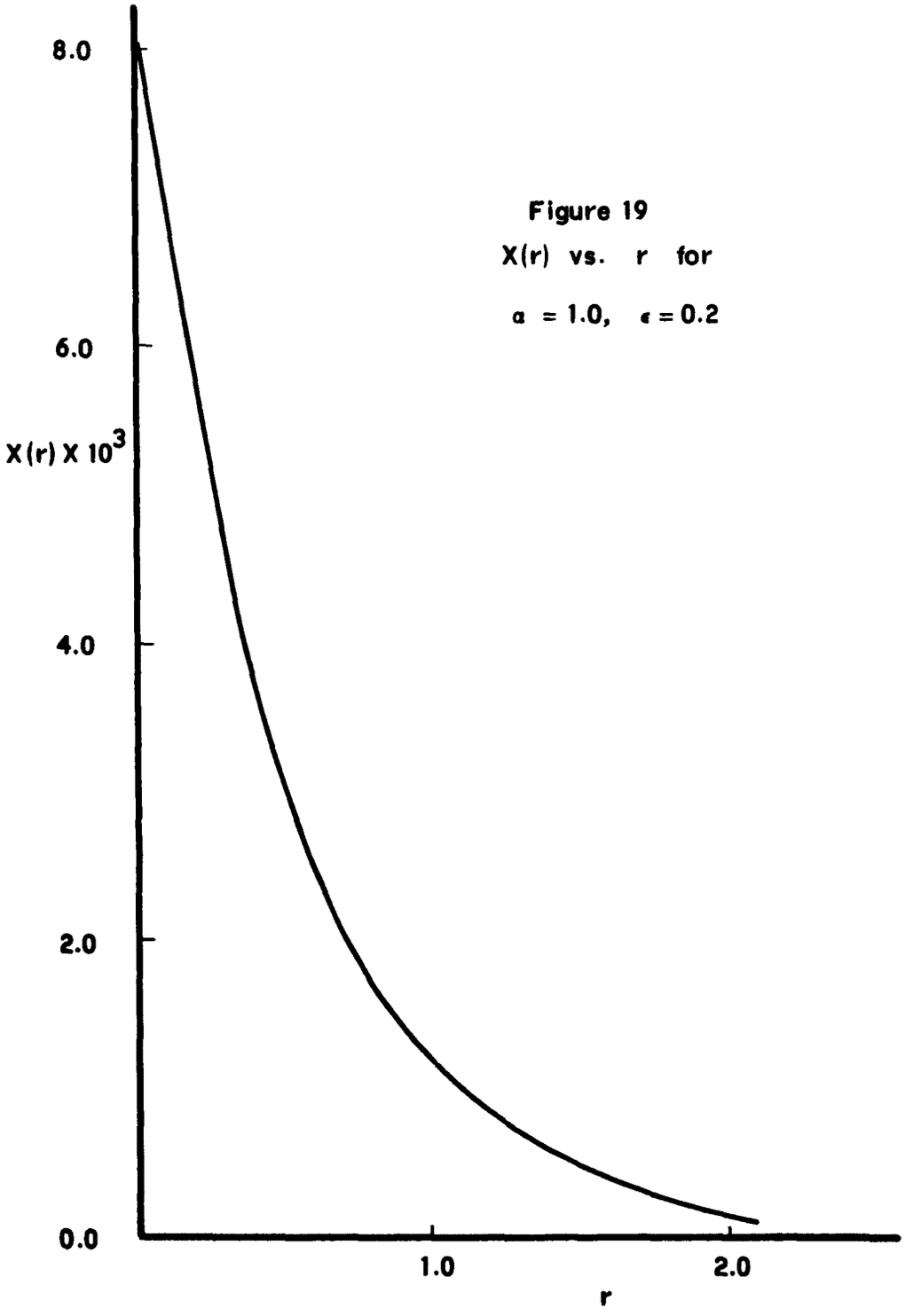

Figure 19

X(r) vs. r for

$\alpha = 1.0, \quad \epsilon = 0.2$

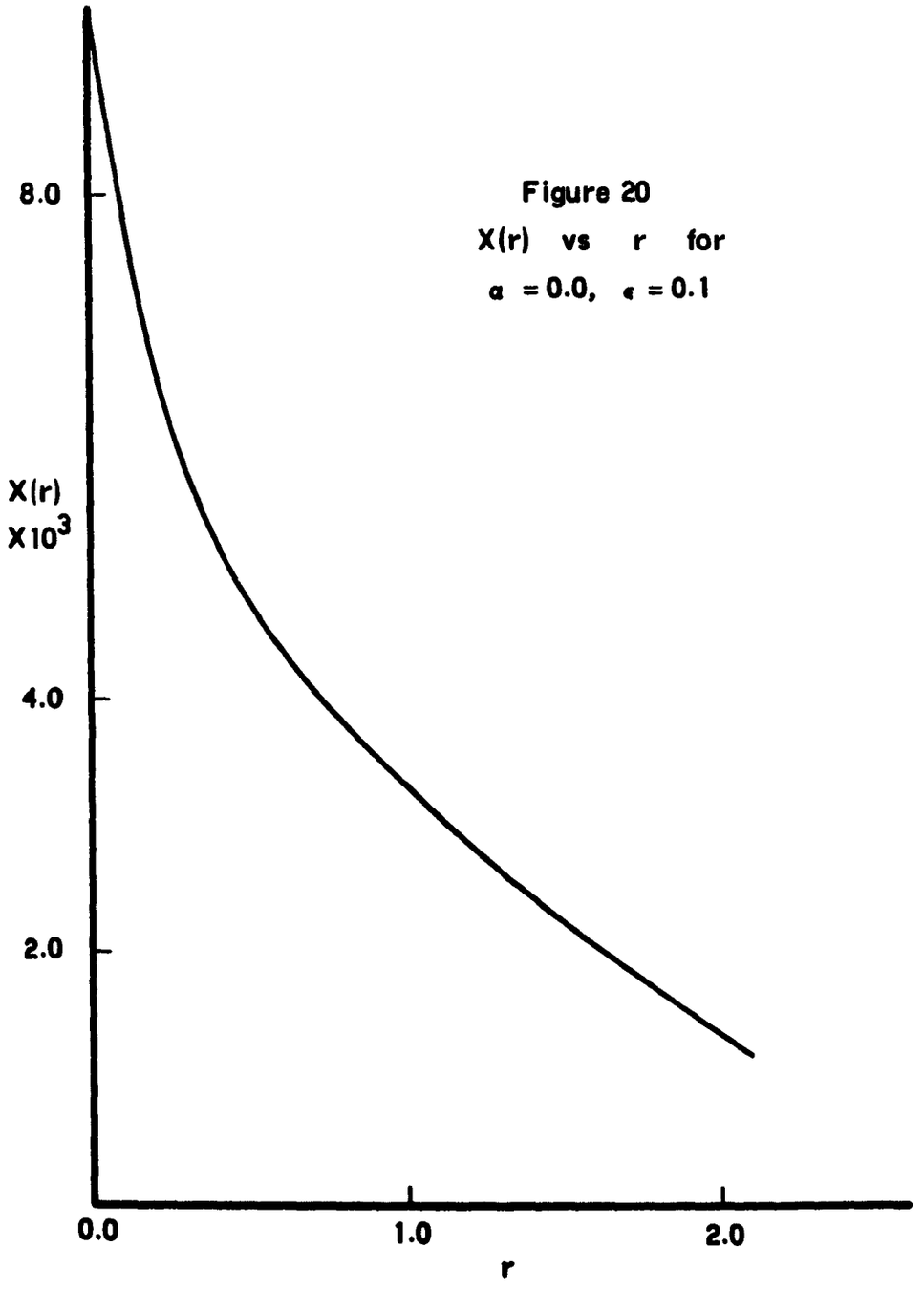

Figure 20
X(r) vs r for
$\alpha = 0.0$, $\epsilon = 0.1$

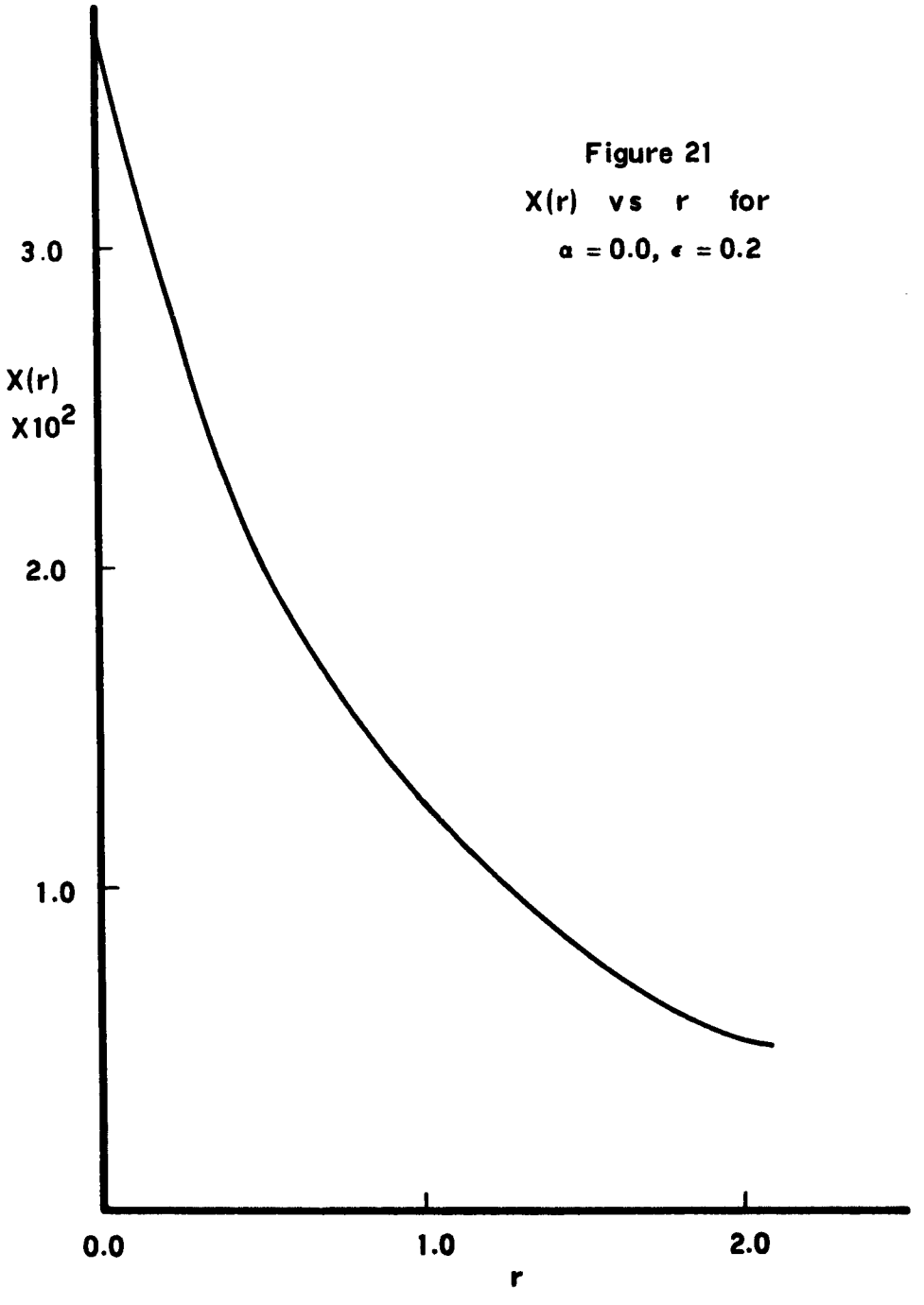

Figure 21
X(r) vs r for
$\alpha = 0.0, \epsilon = 0.2$

VI. CONCLUSIONS

Chapters II, III, IV, have been designed to show the interrelation between the spectral line profile, the electric microfield distribution, and the pair correlation functions or potentials of the mean force; it was seen how the correlation function influences the microfield distribution which in turn modifies the spectral line shape.

In Chapter V the method of correcting the Debye-Hückel pair correlation function was indicated and some aspects of the results were disclosed.

We want to work in reverse in the present chapter, that is, to consider first the implications of Chapter V and then to apply these to a discussion of the preceding chapters. For this purpose, it is found most convenient to consider two-body effects expressed in terms of the potential of the mean force rather than the pair correlation function; this is due to the fact that in Chapter III, it is this quantity, contained explicitly in $\Psi_2(y)$, which finally enters the microfield calculation. First, the potential of the mean force will be considered for the Coulomb example; then, due to its direct application to the quasi-static aspects of the line broadening theory, the case of the shielded potential will be discussed in some detail.

For the Coulomb case, the corrected expression for the potential of the mean force indicates that the Debye-Hückel result overestimates the effective repulsive potential for smaller values of r, while underestimating it at the larger r values: Close interactions are more favored, weak ones, less so. From Figs. 20 and 21, it is seen that the contribution to $w_2(r)$ over the entire r range from the $l - k = 2$ term

is much smaller than that due to the $\ell - k = 1$ term. Even though rigorous proof is missing, the supposition that higher complexity terms ($\ell - k \geq 3$) will be negligible seems reasonable.

The $\epsilon = 0.2$ curve differs from that for $\epsilon = 0.1$ in two respects: (1) the magnitude of its deviation from the Debye-Hückel graph is larger over most of the range of r values, the region of crossover being the only exception; (2) the point at which it crosses the Debye-Hückel curve occurs at a larger value of r.

The shielded-field case provides results which are more interesting than those found in the Coulomb case. A comparison of Fig. 13 and 14 shows that the deviations of the $\epsilon = 0.1, 0.2$ cases from the corresponding Debye-Hückel results are not only different in magnitude, but also in direction; as the parameter ϵ is varied from 0.1 to 0.2, the relative position of the Debye-Hückel graph and the corrected curve reverse. For $\epsilon = .1$ the corrected curve lies above the Debye-Hückel figure thus implying that the latter result underestimates the shielding effects. When $\epsilon = .2$, the correction lies below the Debye-Hückel curve, implying an overestimation of the shielding. For neither value of ϵ does the correction lie equidistant from the Debye-Hückel expression: the percent difference between the graphs is a function of r.

Now let us consider how this behavior of the shielded field might affect the ionic microfield distribution. As was indicated in Chapter III, the low-frequency microfield distribution is strongly dependent upon the nature of the pair correlation function or the potential of the mean force, even though these quantities are much smaller than their companion one-body

terms. Note (see Fig. 3) that the effect of including Debye-Hückel pair correlation is to shift the most probable field strength markedly toward weaker fields, while simultaneously increasing the magnitude of this peak.

It is now possible to conjecture about the effect of the corrected potentials of the mean force on the microfield distribution. In the $\epsilon = .1$ case, the new potential is everywhere greater, which means that all possible fields are slightly less probable than indicated by the Debye-Hückel approximation. Therefore, it would be expected that the corrected microfield distribution would be shifted little if any,

For $\epsilon = .2$, the relative correction becomes larger, as r is increased; thus, although larger fields become a little more likely, the weaker fields are much more probable. The microfield distribution would have its peak slightly lowered and shifted noticeably toward weaker fields, while the strong field wing would be raised a small amount.

It is fully recognized that the above discussion is only supposition, and that the microfield calculation must be carried out for various values before any definite statements can be made. However, the need for such a revised calculation has been demonstrated.

It is interesting to consider further whether it is possible to verify or disprove a given set of microfield calculations. One such possibility exists in the case of the low-frequency or ionic microfield distribution; this involves the shift of spectral line profiles as shown in Chapter II. In order to separate the microfield effect from the other shift-inducing possibilities, we must choose a spectral line for consideration where the desired effect would be expected to be large. With this requirement in

mind, it was first proposed that the shift of the peaks of the Lyman -β line be examined experimentally, and the results compared with those predicted by theory; a typical Lyman β profile is shown in Fig. 22.

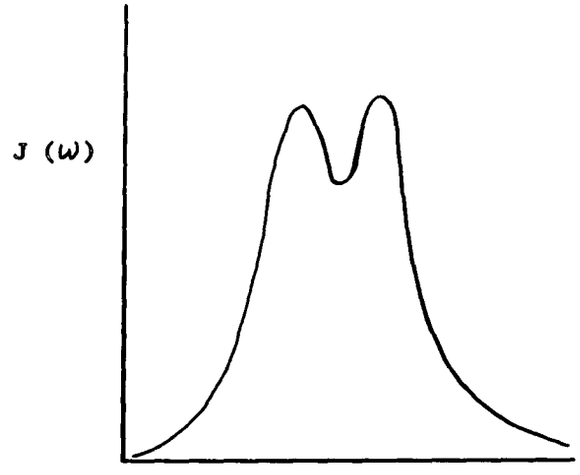

Figure 22 Typical Lyman β Profile

The experimental study of the Lyman β line has recently been done for a given temperature and density condition by Elton.[45] However, his results are not conclusive since the position of the line peaks, strongly affected by self-absorption, do not allow one to discriminate between currently proposed distributions. There is another possibility which also concerns the Lyman β line; in this case the line profile would be determined holding T relatively constant, for several values of density. In this fashion, one should be able to observe the trend in the peak shift. Such an experiment is definitely possible.[48]

It has been established that the correction of the pair correlation function and corresponding potential of the mean force should produce a

considerable change in the electric microfield distribution function calculated using the Debye-Hückel expressions. This change will result in the alteration of spectral line shifts, which, in certain cases, are subject to experimental verification.

APPENDIX A

In the evaluation of the integral in Eq. (5.13), it was stated that the contribution of $\int_{c_2}$ was zero, i.e.,

$$\lim_{R \to \infty} \int_{c_2} \frac{\Gamma(s)\,\Gamma(s+2)\,\sin\left[(s+2)\tan^{-1}(-\frac{b}{as})\right]}{\frac{s+2}{2}} \, ds = 0 \qquad (A.1)$$

$$\left[(as)^2 + b^2\right]$$

It is the purpose of this appendix to verify this assertion.

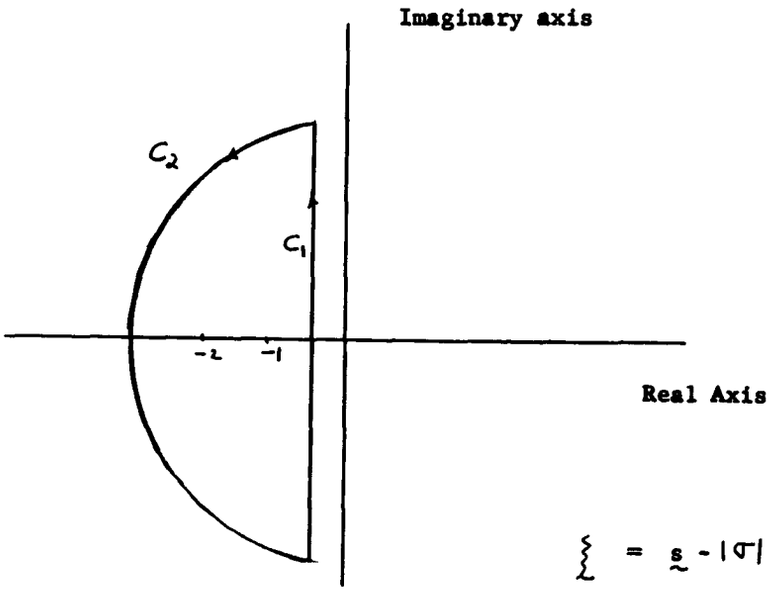

First consider the term:

$$\sin\left[(s+2)\tan^{-1}(-\frac{b}{as})\right] = \sin\left\{\left[(-\frac{b}{as}) - \frac{1}{3}(-\frac{b}{as})^3 + \cdots\right](s+2)\right\} \qquad (A.2)$$

which for large Re s

$$= \sin\left[-\frac{b}{a} + \frac{1}{3} \quad \frac{b^3}{a^3 s^2} + \ldots \right]$$

For Re s $\longrightarrow \infty$

$$\sin\left[(s+2) \tan^{-1}(-\frac{b}{as}) \right] \longrightarrow -\sin\frac{b}{a} \qquad \text{(A.3)}$$

From Sterling's Theorem,

$$\ln\Gamma(s) = \ln(s-1)! \cong (s+\tfrac{1}{2}) \ln(s-1) - (s-1) + \ln\sqrt{2\pi}$$

$$\ln\Gamma(s+2) = \ln(s+1)! \cong (s+3/2) \ln(s+1/2) - (s+1) + \ln\sqrt{2\pi}$$

Therefore,

$$\ln\left[\Gamma(s)\Gamma(s+2)\right] = (s-\tfrac{1}{2}) \ln(s-1) + (s+\tfrac{3}{2}) \ln(s+1)$$

$$- 2s + \ln 2\pi$$

$$\tilde{\cong} (2s+1) \ln s - 2s + \ln 2\pi \qquad \text{(A.4)}$$

or,

$$\Gamma(s)\Gamma(s+2) \tilde{\cong} 2\pi s^{2s+1} e^{-2s} \qquad \text{(A.5)}$$

Also, for large Re s

$$\left[(as)^2 + b^2\right]^{\frac{s+2}{2}} \cong (as)^{s+2} \qquad \text{(A.6)}$$

This implies that for large s,

$$s \cdot \left\{ \frac{\Gamma(s)\,\Gamma(s+2)}{\left[(as)^2+b^2\right]^{\frac{s+2}{2}}} \right\} \cong \frac{2\pi\, s^{2s+2}\, e^{-2s}}{a^{s+2}\, s^{s+2}}$$

$$= \frac{2\pi\, s^{s}\, e^{-2s}}{a^{s}\, 2} \qquad \text{(A.7)}$$

Including the sine term we find that the product of s times the integrand for large values of s becomes

$$s \cdot \text{Integrand} = \frac{2\pi\, s^{s}\, e^{-2s} \sin\left(-\frac{b}{a}\pi\right)}{a^{s}\, 2} \qquad \text{(A.8)}$$

This is in general not equal to zero, which is what must be shown.

After a change of variables from s to $\xi = s - |\sigma|$ we determine the log of $s \cdot I$ and take the real part. This must be equal to $-\infty$ if $\lim_{\xi \to \infty} \int_{c_2} \longrightarrow 0$.

$$\ln\left[\ \right] = 2\pi + (\xi+\sigma)\ln(\xi+\sigma) - 2(\xi+\sigma) - (\xi+\sigma+2)\ln a - \ln\sin\left(-\frac{b}{a}\pi\right)$$

$$\cong \ln 2\pi + (\xi+\sigma)\ln\xi - 2\xi - 2\sigma - (\sigma+2)\ln a - \xi \ln a$$

Let

$$\zeta = R\, e^{i\varphi} = R\left[\cos\varphi + i \sin\varphi\right]$$

Then,

$$\text{Re ln}\left[\ \right] = \left[\ln 2\pi - 2\sigma - (\sigma + 2)\ln a\right]$$
$$+ (R\cos\varphi + \sigma)\ln R - R\varphi\sin\varphi$$
$$- 2R\cos\varphi - R\cos\varphi \ln a$$

For R very large, this reduces to

$$\text{Re ln}\left[s \cdot I\right] = R \ln R \cos\varphi - R\varphi\sin\varphi \qquad (A.9)$$

Subject to the restriction $\frac{\pi}{2} < \varphi < \frac{3\pi}{2}$,

$$\lim_{R \to} \text{Re ln}\left[s \cdot I\right] \longrightarrow -\infty \qquad (A.10)$$

But, this is just the region of integration; hence, Eq. (A.1) is shown to be valid.

APPENDIX B

In Chapter V it was stated that Eq. (5.19) reduced to Bowers' expression for $\alpha = 0$. This will be demonstrated in this appendix.

Setting $\alpha = 0$ in Eq. (5.19) yields,

$$f(k) = -\frac{4\pi\epsilon}{k^2}\left[1 + \sum_{n=2}^{\infty} \frac{(\epsilon k)^{n-1}}{\Gamma(n+1)\,\Gamma(n-1)} \left\{\right\}\right] \qquad (5.20)$$

where

$$\left\{\right\} = \left\{\frac{\pi}{2}\cos\left(\frac{n\pi}{2}\right) + \sin\left(\frac{n\pi}{2}\right)\left[\ln \epsilon k - \psi(n+1) - \psi(n-1)\right]\right\}$$

In order to prove the above assertion, Bowers' result will be shown to be identical to Eq. (5.20). From Chapter V, Bowers' result is

$$f(k) = -\frac{4\pi\epsilon}{k^2} \cdot 2\ \ker_2(\eta) \quad ; \eta \equiv (4\epsilon k)^{\frac{1}{2}} \qquad (5.21)$$

By definition, [38]

$$\ker_2(\eta) = -\mathrm{Re}\left[K_2\left(\eta\, i^{1/2}\right)\right] \qquad (B.1)$$

where K_2 is a modified Bessel function which is defined as

$$K_2(z) = \frac{1}{2}\sum_{r=0}^{1}\frac{(-1)^r(1-r)!}{r!}\left(\frac{2}{z}\right)^{2-2r} - \sum_{r=2}^{\infty}\frac{\left(\frac{z}{2}\right)^{2r+2}}{r!\,(r-2)!}\left[\ln\left(\frac{z}{2}\right) - \frac{1}{2}\left[\psi(r+1) + \psi(r-1)\right]\right] \tag{B.2}$$

In view of B.1 and B.2,

$$2k\,\mathrm{ker}_2(\eta) = 1 + \sum_{2}^{\infty}\frac{\left[\left(\frac{\eta}{2}\right)^2\right]^{r+1}}{\Gamma(r+1)\,\Gamma(r-1)}\left\{\frac{\pi}{2}\cos\left(\frac{r\pi}{2}\right) + \sin\left(\frac{r\pi}{2}\right)\left[\ln\left(\frac{\eta}{2}\right)^2 - \psi(r+1) - \psi(r-1)\right]\right\}$$

Multiplying by $-\frac{4\pi\epsilon}{k^2}$ we find

$$f(k) = -\frac{4\pi\epsilon}{k^2}\cdot 2\,\mathrm{ker}_2$$

$$= -\frac{4\pi\epsilon}{k^2}\left[1 + \sum_{r=2}^{\infty}\frac{(\epsilon k)^{r-1}}{\Gamma(r+1)\,\Gamma(r-1)}\left\{\;\right\}\right]$$

where

$$\left\{\right\} = \left\{\frac{\pi}{2} \quad \cos\left(\frac{r\pi}{2}\right) + \sin\left(\frac{r\pi}{2}\right)\left[\ln\ (\epsilon k) - \psi(r+1) - \psi(r-1)\right]\right\}$$

which is identical to the result derived from Eq. (5.19) by setting $\alpha = 0$.

APPENDIX C

Solution of the expression

$$X(r_{12}) = \rho \int dr_3 \Gamma(r_{13}) \left[\Gamma^2(r_{32}) - f^2(r_{32}) \right] + \frac{\rho^2}{2} \iint dr_3\, dr_4 \Gamma(r_{13}) \left[\Gamma^2(r_{34}) - f^2(r_{34}) \right] \Gamma(r_{42}) \tag{4.43}$$

using the Debye-Hückel expression for Γ, and letting $f = f_o$,

$$\Gamma(r) \cong \Gamma_o(r) = -\frac{\epsilon}{r} e^{-\sqrt{\alpha^2+1}\, r}$$

$$f(r) = f_o(r) = -\frac{\epsilon}{r} e^{-\alpha r} \tag{5.3}$$

It is here convenient to introduce bipolar coordinates, see Fig.(C.1).

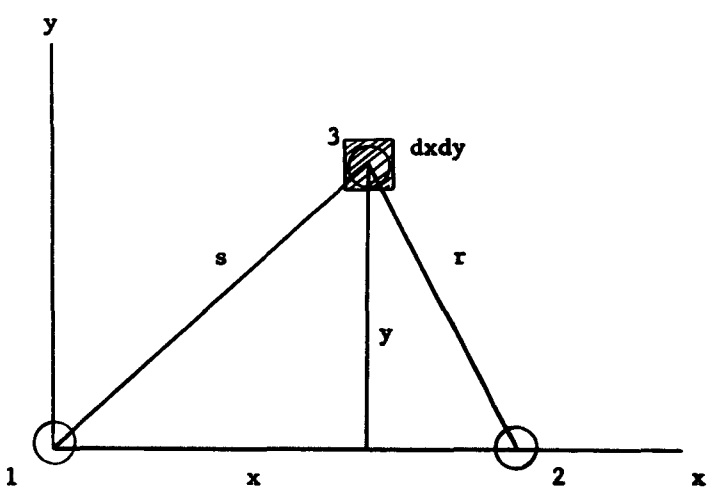

Figure (C.1) Bipolar Coordinates

So $r_{12} \equiv R$, $r_{13} \equiv s$, $r_{23} \equiv r$

$$d^3r_3 = 2\pi y \, dxdy \tag{C.1}$$

Transforming to s, r coordinates, we use the relation

$$dsdr = \begin{vmatrix} \frac{x}{s} & \frac{y}{s} \\ \frac{x-R}{r} & \frac{y}{r} \end{vmatrix} dxdy \tag{C.2}$$

Therefore,

$$d^3r_3 = 2\pi y \, dxdy = \frac{2\pi sr}{R} \, ds \, dr \tag{C.3}$$

First, consider the evaluation of

$$I \equiv \rho \int d^3r_3 \, \Gamma(r_{13}) \left[\Gamma^2(r_{32}) - f^2(r_{32}) \right]$$

$$\Gamma_o(r_{13}) = -\frac{\epsilon}{s} e^{-\sqrt{\alpha^2 + 1}\, s}$$

$$\Gamma_o(r_{32}) = -\frac{\epsilon}{r} e^{-\sqrt{\alpha^2 + 1}\, r}$$

$$f_o(r_{32}) = -\frac{\epsilon}{r} e^{-\alpha r}$$

Before proceeding any further, it should be noted that as in the text, the interparticle distances are given in terms of the Debye length, λ .

A consequence of this is that for every volume element appearing in the integrals to be evaluated, a factor λ^3 must be included. Furthermore, as a result of the definitions (5.2) in the text,

$$\epsilon = \frac{1}{4\pi\rho\lambda^3}$$

or

$$4\pi\rho\epsilon\lambda^3 = 1 \tag{C.4}$$

Using the preceding information and definitions, one has

$$I = \frac{(4\pi\rho\epsilon\lambda^3)\cdot\epsilon^2}{2R}\int_0^{\infty}\frac{1}{r}\left[e^{-2\sqrt{\alpha^2+1}\,r} - e^{-2\alpha r}\right]dr\int_{|R-r|}^{R+r} e^{-\sqrt{\alpha^2+1}\,s}(-ds) \tag{C.5}$$

$$= \frac{\epsilon^2}{2R}\left\{\int_0^{r}\frac{1}{r}\left[e^{-2\sqrt{\alpha^2+1}\,r} - e^{-2\alpha r}\right]dr\int_{R-r}^{R+r} e^{-\sqrt{\alpha^2+1}\,s}\left(-\sqrt{\alpha^2+1}\,ds\right)\right.$$

$$\left. + \int_R^{\infty}\frac{1}{r}\left[e^{-2\sqrt{\alpha^2+1}\,r} - e^{-2\alpha r}\right]dr\,\frac{1}{\sqrt{\alpha^2+1}}\int_{r-R}^{r+R} e^{-\sqrt{\alpha^2+1}\,s}\left(-\sqrt{\alpha^2+1}\,ds\right)\right\} \tag{C.6}$$

$$I = \frac{\epsilon^2}{2\sqrt{\alpha^2+1}\,R}\left\{ e^{-\sqrt{\alpha^2+1}\,R}\int_0^R \frac{1}{r}\left[e^{-\sqrt{\alpha^2+1}\,r} - e^{-2\alpha r}\right]\left[e^{-\sqrt{\alpha^2+1}\,r} - e^{+\sqrt{\alpha^2+1}\,r}\right]dr \right.$$

$$\left. + (e^{-\sqrt{\alpha^2+1}\,R} - e^{+\sqrt{\alpha^2+1}\,R})\int_R^\infty \frac{1}{r}\left[e^{-2\sqrt{\alpha^2+1}\,r} - e^{-2\alpha r}\right] e^{-\sqrt{\alpha^2+1}\,r}\,dr \right.$$

If one pursues this calculation further and in doing so introduces the functions

$$E_-(R) = \int_R^\infty \frac{e^{-r}}{r}\,dr \qquad (C.7)$$

$$E_1(R) = \int_{-R}^\infty \frac{e^{-r}}{r}\,dr \qquad \text{, a final expression}$$

for I (R) can be found:

$$I(R) = \frac{\epsilon^2}{2\sqrt{\alpha^2+1}\,R}\left[e^{-\sqrt{\alpha^2+1}\,R}\left\{\ln\left(\frac{1}{3}\,\frac{2\alpha+\sqrt{\alpha^2+1}}{2\alpha-\sqrt{\alpha^2+1}}\right) + E_-(\sqrt{\alpha^2+1}\,R) - E_-\left[(2-\sqrt{\alpha^2+1})R\right]\right\}\right. \qquad (C.8)$$

$$\left. + e^{+\sqrt{\alpha^2+1}\,R}\left\{E_-\left(2\alpha+\sqrt{\alpha^2+1}\right)R - E_-(3\sqrt{\alpha^2+1}\,R)\right\}\right]$$

Now the second integral to be evaluated is, II,

$$II = \frac{\rho^2}{2} \int d^3r_4 \, \Gamma(r_4) \int d^3r_3 \, \Gamma(r_{13}) \left[\Gamma^2(r_{34}) - f^2(r_{34}) \right] \qquad (C.9)$$

It will be noticed that the second integral in this expression is equal to $I(r_{14})/\rho$, so

$$II = \frac{\rho}{2} \int I(r_{14}) \, \Gamma_o(r_{42}) \, d^3r_4 \qquad (C.10)$$

Again, using bipolar coordinates,

$$r_{14} \equiv s$$

$$r_{42} \equiv r$$

$$d^3r_4 = \frac{2\pi sr}{R} \, ds \, dr \qquad (C.11)$$

Therefore,

$$II = \frac{\pi\rho}{R} \int I(s) \, sds \int \Gamma_o(r) \, r \, dr \qquad (C.12)$$

Making the appropriate substitutions and carrying out the rather complicated

calculation, an expression for II (R) is determined:

$$II = \frac{\epsilon^2}{8(\alpha^2+1)R}\left\{e^{-\sqrt{\alpha^2+1}\,R}\left[\frac{2\sqrt{\alpha^2+1}-2\alpha}{6\alpha\sqrt{\alpha^2+1}+3\alpha^2+3}\right.\right.$$

$$-\left(R-\frac{1}{\sqrt{\alpha^2+1}}\right)\left(\ln\left[\frac{1}{3}\cdot\frac{2\alpha+\sqrt{\alpha^2+1}}{2\alpha-\sqrt{\alpha^2+1}}\right]+E_{-}(\sqrt{\alpha^2+1}\,R)-E_{-}[(2\alpha-\sqrt{\alpha^2+1})R]\right) \qquad (C.13)$$

$$\left.-\frac{1}{2\alpha-\sqrt{\alpha^2+1}}\left(e^{-(2\alpha-\sqrt{\alpha^2+1})R}-1\right)+\frac{1}{\sqrt{\alpha^2+1}}\left(e^{-\sqrt{\alpha^2+1}\,R}-1\right)\right]$$

$$-e^{+\sqrt{\alpha^2+1}\,R}\left[\left(R+\frac{1}{\sqrt{\alpha^2+1}}\right)\left(E_{-}(3\sqrt{\alpha^2+1}\,R)-E_{-}(2\alpha+\sqrt{\alpha^2+1})R\right)\right.$$

$$\left.\left.-\frac{1}{2\alpha+\sqrt{\alpha^2+1}}e^{-(2\alpha+\sqrt{\alpha^2+1})R}+\frac{1}{3\sqrt{\alpha^2+1}}e^{-3\sqrt{\alpha^2+1}\,R}\right]\right\}$$

Thus,

$$X(R) = I(R) + II(R)$$

$$X(R) = \frac{\epsilon^2}{8(\alpha^2+1)R}\left\{e^{-\sqrt{\alpha^2+1}\,R}\left[\frac{2\sqrt{\alpha^2+1}-2\alpha}{6\alpha\sqrt{\alpha^2+1}+3\alpha^2+3}\right.\right.$$

$$\left.-\left(R-\frac{4\alpha^2+3}{\sqrt{\alpha^2+1}}\right)\left(\ln\left[\frac{1}{3}\cdot\frac{2\alpha+\sqrt{\alpha^2+1}}{2\alpha-\sqrt{\alpha^2+1}}\right]+E_{-}(\sqrt{\alpha^2+1}\,R)-E_{-}(2\alpha-\sqrt{\alpha^2+1})R\right)\right.$$

$$- \frac{1}{2\alpha - \sqrt{\alpha^2+1}} \left(e^{-(2\alpha - \sqrt{\alpha^2+1})R} - 1 \right) + \frac{1}{\sqrt{\alpha^2+1}} \left(e^{-\sqrt{\alpha^2+1}\,R} - 1 \right) \Bigg] \qquad \text{(C.14)}$$

$$- e^{+\sqrt{\alpha^2+1}\,R} \Bigg[\left(R + \frac{4\alpha^2+3}{\sqrt{\alpha^2+1}} \right) \left(E_-(3\sqrt{\alpha^2+1}\,R) - E_-(2\alpha + \sqrt{\alpha^2+1})R \right)$$

$$+ \frac{1}{2\alpha + \sqrt{\alpha^2+1}} e^{-(2\alpha + \sqrt{\alpha^2+1})R} - \frac{1}{3\sqrt{\alpha^2+1}} e^{-3\sqrt{\alpha^2+1}\,R} \Bigg] \Bigg\}$$

APPENDIX D

The machine calculations for the work reported here were performed on an LGP-30 computer.

The numerical work may be separated into two steps: (1) the calculation of f (k), and (2) the evaluation of $\Gamma(r)$.

1. Calculation of f (k)

From equation Chapter V,

$$f(k) = -\frac{4\pi\epsilon}{k^2}\left[1 + \sum_{n=2}^{\infty} \frac{(\epsilon k)^{n-1}}{\Gamma(n+1)\Gamma(n-1)}\left\{\right\}\right] \tag{5.20}$$

$$\left\{\right\} = \left\{\frac{\pi}{2}\cos\left(\frac{n\pi}{2}\right) + \sin\left(\frac{n\pi}{2}\right)\left[\ln(\epsilon k) - \psi(n+1) - \psi(n-1)\right]\right\}$$

This is the expression derived from equation (5.19) for $\alpha = 0$; the remarks to be made in this appendix will also apply to the more general result.

In carrying out the computer calculation, some problems were encountered which are worthy of note; in order to establish a series cutoff criterion, it was specified that when a term contributed less than 0.1% to the preceding summation, the series was to be terminated. However, upon attempting to verify this step it was found that it is necessary to require that not one, but two successive terms be less than 0.1% before termination is accomplished; this requirement is due to the oscillatory nature of the series terms.

An additional feature of the f (k) computation which should also be noted is that for large values of k, f (k) becomes very small and if

accuracy is to be maintained, care must be taken to assure that sufficient terms are included in the series.

2. Evaluation of $\Gamma(r)$.

From Chapter V we have,

$$\Gamma(r) = \frac{1}{2\pi^2 r} \int_0^\infty d\,k\,k\,\sin(k\,r) \left[\frac{f(k)}{1 - \rho f(k)} \right] \tag{5.23}$$

In performing this evaluation, tabulated values of f (k) were employed. The initial attempt at this computation involved the generation of sufficient f (k) vs k points to allow a smooth curve to be drawn. From this curve, additional values of f (k) were determined by means of interpolation; these values along with those actually generated by the computer were used in the tabulation. Subsequent investigation disclosed that $\Gamma(r)$ was extremely sensitive to the accuracy of the tabulated f (k) values. A detailed study was then conducted to ascertain the number of generated points necessary to insure the desired accuracy.

An additional independent study was made to evaluate the affect of various Δk increments on the $\Gamma(r)$ computation. Finally, the expression for $\Gamma(r)$ was carried out to the point where additional integration increments contributed less than 1.0%.

It was stated in the text that the numerical work of Bowers was considered incorrect. In his paper[52] he specified that tabulated values of $\ker_2(\eta)$ were used in his calculations; the tables he referenced were: Tables of Integrals, by H. B. Dwight, The Macmillan Co., New York, 1949.

These tables only provide ten points on an f (k) curve. It has been clearly established, during the course of the present work, that the Bowers' treatment is incorrect.

BIBLIOGRAPHY

1. B. Mozer and M. Baranger, Phys. Rev. 115, 521 (1959); Phys. Rev. 118, 626 (1960).
2. E. E. Salpeter, Ann. Phys. 5, 183 (1958); and
3. T. L. Hill, Statistical Mechanics, McGraw-Hill Co., New York, 1956.
4. J. Holtsmark, Physik, Z. 20, 162 (1919); Ann der Physik 58, 577 (1919); Physik, Z. 25, 73 (1924).
5. M. Baranger, Phys. Rev. 111, 494 (1958); ibid., 111, 481 (1958); ibid., 112, 855 (1958).
6. A. Kolb and H. Griem, Phys. Rev. 111, 514 (1958).
7. S. Ch'en and M. Takeo, Rev. Modern Phys. 29, 20 (1957).
8. R. G. Breene, Rev. Modern Phys. 29, 94 (1957).
9. H. Margenau and M. Lewis, Rev. Modern Phys. 31, 569 (1959).
10. L. Landau and E. Lifshitz, The Classical Theory of Fields, (Addison-Wesley Press, Inc., Reading Mass., 1951), p. 193.
11. P. W. Anderson, Phys. Rev. 76 647 (1949).
12. S. Chandrasekhar, Rev. Modern Phys. 15, 1 (1943).
13. E. B. Turner, The Production of Very High Temperatures in the Shock Tube with an Application to the Study of Spectral Line Broadening, AFOSR TN 56-150, ASTIA Document No. AD86309, Univ. of Mich. Eng. Res. Inst. (1956)
14. A. C. Kolb, Theory of Hydrogen Line Broadening in High-Temperature Partially Ionized Gases, AFOSR TN 57-8, ASTIA Document No. AD115040, Univ. of Mich. Eng. Res. Inst. (1957).

15. H. Griem, Z. Physik 137, 280 (1954).

16. M. Baranger, Phys. Rev. 91, 436 (1953).

17. G. Ecker, Z. Physik 148, 593 (1957); and K. G. Muller, Z. Physik 153, 317 (1958).

18. H. Hoffman and O. Theimer, Astrophys. J. 127, 477 (1958);

19. H. Griem, A. C. Kolb, and K. Shen, Phys. Rev. 116, 4 (1959).

20. A. A. Broyles, Phys. Rev. 100, 1181 (1955); Z. Physik 151, 187 (1958).

21. M. Lewis and H. Margenau, Phys. Rev. 109, 842 (1958).

22. M. G. Mayer and J. E. Mayer, Statistical Mechanics, (John Wiley and Sons, Inc., New York, 1940), Chap. 13.

23. J. E. Mayer and E. Montroll, J. Chem. Phys. 9, 4 (1941).

24. D. ter Haar, Elements of Statistical Mechanics, (Rinehart and Co., Inc., New York, 1956), p. 173.

25. P. Debye and E. Huckel, Physik, Z. 24, 185 (1923).

26. D. Pines and D. Bohm. Phys. Rev. 85, 338 (1952).

27. L. Landau and E. Lifshitz, Statistical Physics, (Pergamon Press Ltd., London, 1958), sec. 74.

28. P. M. Morse, Vibration and Sound (McGraw-Hill Book Company, Inc., New York, 1946), pp. 316-317.

29. E. T. Whittaker and G. N. Watson, Modern Analysis, (University Press, Cambridge, 1952), Chap. XVII.

30. D. Pines, Solid State Physics I, (Academic Press, Inc., New York, 1955), p. 445.

31. E. W. Montroll, La Theorie des Gaz Neutres et Ionises, John Wiley and Sons, Inc., New York, 1959.

32. J. G. Trulis and S. G. Brush, Phys. Rev. 121, 940 (1961).

33. R. Abe, Prog. Theor. Phys. 22, 213 (1959).

34. T. Morita and K. Hiroike, Prog. Theor. Phys. 23, 385 (1960).

35. E. Meeron, Phys. of Fluids 1, 139 (1958).

36. E. Meeron, Physics 26, 445 (1960).

37. A. Ron and G. Kalman, Phys. Rev. 123, 1100 (1961).

38. N. W. McLachlan, Bessel Functions For Engineers, Clarendon Press, Oxford, 1934.

39. W. Grobner and N. Hofreiter, Integraltafel, Zweiter Teil, Bestimmte Integrale, Springer-Verlag, Wen and Innsbruck, 1950.

40. Tables of the Exponential Function e^x, National Bureau of Standards, 1939.

41. G. Sansone and J. Gerretsen, Lecutres on the Theory of Functions of a Complex Variable, I. Holomorphic Functions, P. Noordhoff, Ltd., Groningen, The Netherlands, 1960.

42. Tables of Sine, Cosine and Exponential Integrals, Vol. I and II, National Bureau of Standards, 1940.

43. E. C. Titchmarsh, Introduction to the Theory of Fourier Integrals, Clarendon Press, Oxford, 1937.

44. G. N. Watson, A Treatise on the Theory of Bessel Functions, Macmillan Co., New York, 1945.

45. R. C. Elton, Stark Profile Measurements of the Ly-α and Ly-β Lines of Hydrogen, Dissertation, University of Maryland, 1963.

46. H. R. Griem, et al., Phys. Rev. 125, 177 (1962)

47. J. E. Mayer, J. Chem. Phys. 18, 1426 (1950)

48. H. R. Griem, Private Communication.

49. S. Chandrasekhar, Rev. Mod. Phys. 15, 1 (1943)

50. W. G. McMillan, Jr., and J. E. Mayer, J. Chem. Phys. 13, 276 (1945).

51. M. Baranger, Atomic and Molecular Processes, edited by D. R. Bates, Academic Press, New York, 1962, Ch. 13.

52. D. L. Bowers, Phys. Rev. 119, 1180 (1960).

53. L. Spitzer, Jr., Physics of Fully Ionized Gases, Interscience Publishers, Inc., New York, 1956.

ERRATA

Page	Location	Item
28	Eq. (3.16a)	Read $\exp(-\frac{r_{12}}{\lambda/\sqrt{2}})$ instead of $\exp(-\frac{r_{12}}{\lambda\sqrt{2}})$
45	Line 1	The sentence beginning at the end of this line should read: Each term in this expansion can be represented graphically by a diagram which consists of a system of points representing particles, and a number of connecting lines each of which corresponds to a factor $f(r_{ij})$; the total number of connecting lines in the graph equals the number of factors, $f(r_{ij})$, in the particular term under consideration.
52	Line 18	$(\rho r_M)^3$ should read $(\rho r_M^3)^k$
57	Line 1	$4\pi\epsilon\rho = 1$ should read $4\pi\epsilon\rho\lambda^3 = 1$
70	Eq. (5.20)	$[\ln(\mathfrak{C}k) - \Gamma(n+1) - \Gamma(n-1)]$ should read $[\ln(\mathfrak{C}k) - \Psi(n+1) - \Psi(n-1)]$
88	Lines 15 and 17	Interchange the words <u>overestimates</u> and <u>underestimates</u>
89	Line 8	The sentence beginning on this line should read: Therefore, it would be expected that the corrected microfield distribution would be shifted little if any, but that the peak would be raised and the distribution narrowed slightly.
101	Eq. (C. 6)	Insert the factor $\frac{1}{\sqrt{(\alpha^2+1)}}$ in front of the first integral inside brackets; change the upper limit of integration in this integral from r to R.